**Inês Simões
Peres**

# Development of a prototype for sensing bone-implant interface

Desenvolvimento de protótipo para sensorização da interface de implantes ósseos

Inês Simões
Peres

# Development of a prototype for sensing bone-implant interface

Desenvolvimento de protótipo para sensorização da interface de implantes ósseos

**o júri / the jury**

presidente / president

**Prof. Doutor António Manuel de Amaral Monteiro Ramos**
Professor Auxiliar da Universidade de Aveiro

**Prof. Doutor Manuel José Cabral dos Santos Reis**
Professor Associado com Agregação do Departamento de Engenharias, Escola de Ciências e Tecnologia da *Universidade de Trás-os-Montes e Alto Douro*

**Prof. Doutor Jorge Augusto Fernandes Ferreira**
Professor Auxiliar da Universidade de Aveiro (orientador)

**agradecimentos / acknowledgements**

**keywords**    Bone-implant interface, Instrumented implant, Aseptic loosening, Capacitive sensor

**abstract**    Over the last few years there has been an increase in the number of arthroplasties performed worldwide. With the growing number of young patients performing this surgery, new technologies are required to evaluate the bone-implant interface in order to avoid revision surgeries. The present work aims to develop a prototype for sensing the bone-implant interface for multifunctional instrumented/bioelectronic implants: the network-based cosurface capacitive system with ability to be extracorporeally controlled by clinicians. This prototype is composed by both hardware and software components. The hardware can also be seen as the data acquisition system and the software is the monitor and the control system. Considering that the societal scenario did not allow the manufacture of this new system prototype, the hardware was only designed for future implementation and validation. The software is a web application that allows the clinician to monitor and control the data acquisition system. For the development of the web application it was used Django, python, HTML5, CSS, and the storage and management of data were performed with MySQL. In order to assess its performance, different simulation tests were performed: (i) monitoring tests using random bone-implant interface states, in which capacitance data was generated from a polynomial function that characterizes the average capacitance change for different bone-implant bonding states; (ii) monitoring tests simulating an increasing bonding scenario. Through the web application it is possible to analyse the data collected from the data acquisition system in two dimensional plots or three dimensional plots. This software solution was also designed to allow downloading the data to an Excel file to give the user the possibility to perform different analyses related bone-implant interface state. The project for the data acquisition system is constituted by a Raspberry Pi, an $I^2C$ multiplexer, a capacitor-to-digital converter (EVAL AD-7746), and the sensing technology. The Raspberry Pi is responsible for the TCP-IP communication with the monitoring system and the $I^2C$ communication with the capacitor-to-digital converter through the $I^2C$ multiplexer. It is also responsible for saving data in the correct database. The capacitor-to-digital converter acquires the data from the sensing technology, which is based on three different printed circuit boards, containing twelve capacitors. Thus, it is intended to prove that with a sensing system comprising a network of cosurface capacitors it is possible to acquire bone-implant interface bonding during the daily life of patients, including region and magnitude debonding data.

**resumo**                      Ao longo dos últimos anos tem-se verificado um aumento do número de
                                artroplastias realizadas mundialmente. Com o crescente número de jovens
                                a serem submetidos a esta cirurgia, torna-se necessário desenvolver novas
                                tecnologias para a avaliação da interface osso-implante de modo a diminuir
                                o número de cirurgias de revisão. O presente trabalho tem como objetivo
                                o desenvolvimento de um protótipo para a sensorização da interface de
                                implantes ósseos para incorporar implantes instrumentados, constituídos por
                                uma rede de sistemas capacitivos e com a possibilidade de ser controlada
                                extracoporealmente por médicos especializados. O protótipo é constituído
                                por componentes de hardware e software. O hardware consiste no sistema
                                de aquisição de dados e o software permite o controlo e monitorização do
                                hardware. Considerando o estado social atual não foi possível produzir o
                                protótipo deste novo sistema de monitorização, por esse motivo o hardware
                                foi apenas projetado de forma a ser implementado e validado futuramente.
                                O software é uma aplicação web que permite que o médico especialista
                                monitorize o sistema de aquisição de dados. Para o desenvolvimento
                                deste software foi utilizado Django, python, HTML5, CSS, e a gestão e
                                armazenamento de dados foi feita através do MySQL. A validação das
                                funcionalidades do software foi realizada através de dois testes diferentes:
                                (i) testes de monitorização com base em estados aleaórios da interface
                                osso-implante, onde os valores de capacidade foram obtidos com base numa
                                polinomial que caracteriza a variação de capacidade para diferentes estados
                                de ligação osso-implante; (ii) simulação de um teste de aproximação do
                                osso à estrutura capacitiva. Através da aplicação web, é possível visualizar
                                os resultados obtidos a partir de gráficos tridimensionais e bidimensionais.
                                O website também permite o download de um ficheiro Excel com os dados
                                adquiridos, para o utilizador realizar análises independentes relacionadas com
                                o estado da interface osso-implante. O projeto do sistema de aquisição de
                                dados é constituído por um Raspberry Pi, um multiplexer $I^2C$, um conversor
                                analógico-digital (EVAL-AD7746) e o sistema de sensorização. O Raspberry
                                Pi estabelece uma comunicação TCP-IP com o sistema de monitorização
                                e uma comunicação $I^2C$ com o conversor analógico-digital através de um
                                multiplexer $I^2C$. Este dispositivo guarda os dados recolhidos em bases de
                                dados. O conversor analógico-digital recolhe os dados do sistema capacitivo
                                de sensorização, que é constituído por três placas de circiuito impresso, onde
                                cada uma contém um total de doze condensadores. Assim, pretende-se
                                comprovar que com um sistema constituído por uma rede de condensadores
                                é possível fazer uma aquisição de dados relativamente ao estado da interface
                                osso-implante durante o dia-a-dia do paciente.

*"You can't stop the waves but you can learn to surf."*

**Jon Kabat-Zinn**

# Contents

# List of Figures

# List of Abbreviations

**AE** Acoustic Emission.

**CT** Computed Tomography.

**IP** Internet Protocol.

**MRI** Magnetic Resonance Imaging.

**NJR** National Joint Registry.

**OA** Osteoarthritis.

**PCB** Printed Circuit Board.

**PET** Positron Emission Tomography.

**SPECT** Single-photon Emission Computed Tomography.

**THA** Total Hip Arthroplasty.

**TJR** Total Joint Replacement.

# Chapter 1

# Introduction

Arthroplasties, which consist in a reconstructive procedure that alters the structure of a joint, are one of the most common surgical procedures performed worldwide, accounted for more than a million replacement surgeries every year [1].

This number is expected to double in the next two decades, due to the ageing population and obesity [1]. Although this surgery has excellent outcomes, hip and knee revision surgeries are still required in 6.45% of the cases after five years and 12.9% after ten years [2]. Surgical revisions of joint replacement are more complex and invasive than the primary replacements [3].

Bone loss is a disorder that leads to unstable bone-implant fixations. Aseptic loss is the main reason for implant failure that occurs when there is an adverse bone remodelling. Aseptic loosening results of inadequate initial fixation or biologic loss of fixation caused by particle-induced osteolysis around the implant [4]. Many efforts have been made to study this issue and new implant technologies emerged in the scientific community.

## 1.1   Joint replacement

The increase in demand for both knee and hip replacements in US will be 673% and 174% by 2030, respectively [5]. These numbers may be related to the increase in average life expectancy in developed countries, as well as obesity and the population's sedentary life [1, 6]. Over the last decade, the incidence of Total Joint Replacement (TJR) has increased among old ($> 65$ years) and young patients ($< 65$ years) [7].

The main cause for replacement surgery is osteoarthritis [8]. X-ray diagnosis detects that this issue affects more than 50% of the population older than 75 years, but the same diagnosis made with Magnetic Resonance Imaging (MRI) increases this number to more than 89% of population older than 50 years [9]. The increase in the number of diseases that affect bone quality and density causes an increase in bone diseases in the younger population which can lead to arthroplasties. The increase of young patients having arthroplasties causes an increase of revision surgeries, due to their higher activity and obesity levels [7]. Common causes in all patients that may also lead to revision surgery are aseptic loosening, instability, periprosthetic fracture, prosthetic failure, stiffness or pain [1, 6].

## 1.2   Osteoarthritis

Osteoarthritis (OA) is the most common type of arthritis. OA occurs when the cartilage gradually deteriorates. This disease is associated with multiple risk factors: (i) age: the risk of OA increases with age; (ii) sex: OA is more common in females; (iii) obesity: extra body weight increases the stress in joints, specially hip and knee; (iv) overuse: when the same joint is regularly used, in job or sport; (v) weak muscles: can not support joints in the right position; (vi) genetics.

In the early stages of this condition (Figure 1.1), it is possible to reduce pain with analgesics and other drugs or with non-drug therapies (exercise and weight loss). With time, symptoms may become disabling in such a way that the patient's life can be affected leading to surgery, namely arthroplasties.
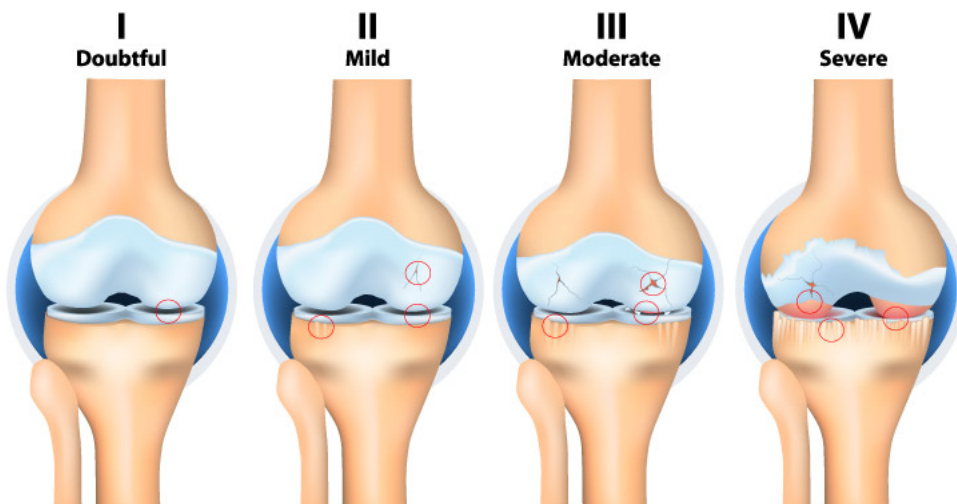


Figure 1.1: Stage of knee osteoarthritis.(from *www.myarthritisrx.com*).

## 1.3   Failure in Implants

The success of an implant depends on several factors. Some of these factors are intrinsic to the prosthesis, such as geometry, materials and surface coating while other factors may be related to the surgical technique and/or the surgeon's experience [10].

There are different types of surgery for different types of implants (cemented, cementless and hybrid) each one with advantages and disadvantages, but all of them need an appropriate fixation. In the last 10 years, an increase about 13.6% in the number of revisions was reported by the Swedish Orthopedic Register [11]. Many studies were performed in order to identify which is the main cause for implant failure that can lead to revision surgery. Rory Ferguson *et al.* [12], identified aseptic loosening (48%) as the main reason for revision surgery followed by dislocation (15%), periprosthetic fracture (10%), infection (9%) and implant malpositioning (5%).

Robert Pivec *et al.* [13], focused their analysis in Total Hip Arthroplasty (THA) and indicated that the most common cause for revision surgery was instability (22%), followed

by mechanical loosening (20%), infection (15%), implant failure (10%), osteolysis (7%), and periprosthetic fracture (6%).

After knee replacement surgery, there is an apparent inverse relation between risk of revision and age: the younger the patient, the higher the risk of revision, where aseptic loosening is responsible for more than 30% of all revisions [14].

The latest report from the National Joint Registry (NJR), which analyses data from England, Wales, Northern Ireland and Isle of Man, reports the most common causes as aseptic loosening (24.3%), dislocation(17.1%) and infection (14.5%) [15].

Aseptic loosening occurs due to the combination of chemical, mechanical and biological factors. Stress shielding is seen as a mechanical failure and corresponds to a reduction in the load transmitted to the bone after stem implantation, leading to peri-implant bone loss that subsequently causes instability for the stem [16]. Corrosion of the metallic components of the implant can lead to the release of compounds that can potentiate inflammation and decrease bone integration. The prosthetic debris is attacked by the human immune system in order to eliminate them. During this process some bone cells are eliminated, eventually causing aseptic loosening for biological reasons.

## 1.4   Types of implants

The healthy tissues of the human body can be destroyed by pathological processes. In advanced stages of these conditions, it may be necessary to replace these tissues with an artificial structure, the bone implants. Implants must be manufactured with biomaterials. A biomaterial should exhibit the following properties (i) biocompatible chemical composition to avoid adverse tissue reactions; (ii) resistance to degradation; (iii) strength to sustain cyclic loading endured by the joint; (iv) minimize bone resorption; (v) high wear resistance to minimize wear-debris generation [17].

The number of arthroplasties procedures made in young people will increase in the next decades [7, 18]. In order to minimize revision surgery rates, aseptic loosening and wear, new design and new materials have been studied. New types of implants are also being developed to overcome this issue. Technological advance enables the development of new implants with a monitoring system to follow implant loosening states.

### 1.4.1   Non-instrumented implants

The first type of implant used in the world was a non-instrumented passive implant made of ivory and it was introduced by Professor Themistocles Gluck [19].

Since the creation of this concept, several types of metallic, polymeric and ceramic materials have appeared for the development of prosthesis [20]. Austenitic stainless steel implants have low resistance to wear [20, 21], which led to a decrease in their use, especially when metallic alloys based on titanium and cobalt chromium appeared. Cobalt chromium alloys have a modulus of elasticity superior than the bone, which causes stress-shielding [20, 21]. In recent years there has been an increase in the use of ceramic materials for the manufacture of prosthesis [22]. One of the first applications of bioceramics consisted in replacing the traditional metal femoral heads of hip prosthesis with high-density and highly pure alumina. With regard to ceramic materials, they have greater resistance to wear and friction [20]. Polymeric materials have also been

used due to their resistance to erosion, biocompatibility, bio-stability and ease of manufacture [20, 23].

Advances in the development of biomaterials have led to the emergence of active non-instrumented implants. These implants are made up of bioactive materials that allow stimulation at the molecular level to promote osseointegration, reduce friction, wear and corrosion. These materials combined with the use of drugs can prevent and reduce infections.

Concerning the fixation method they are distinguished by cement or cementless implants, having advantages and disadvantages in both technologies (Figure 1.2).

Coating the cementeless implant surface with a bioactive material or a porous material can allow bone growth and osseointegration [24]. This process demands a huge bone-implant interaction, so the post-operation recovery is longer and requires less activity. After this recovery time this implants have better results in young patients with a more active lifestyle. Stress-shielding is a disadvantage of this type of implants and it can lead to a decrease in bone density.

Cement implants provide an immediate post-operation fixation, hence it requires less recovery time. Due to their fixation proprieties, it is vulnerable to fatigue failure. This problematic makes this type of devices a better choice for less active people. In addition, this implant is more expensive and the surgical procedure is harder to perform.



Figure 1.2: Cement and cementless implants for primary hip prosthesis (from *www.medicalexpo.com*).

### 1.4.2 Instrumented implants

The lifetime of an implant remains a barrier to be overcome. In order to achieve this goal, the concept of instrumented implant has emerged in recent years. This type of implant has the particularity of allowing the monitoring of some biomechanical properties, such as loads, moments and temperatures.

The first time that *in vivo* data from an implant were collected was in 1966 by Rydell *et al.* [25] who recorded information about the forces and moments applied to the femoral head of a hip prosthesis.

Although this first concept was quite invasive, there was a trigger for new types of instrumented implants, less invasive, without wires for data transmission. These implants can be classified into two categories: active and passive.

**Instrumented passive implants**

A passive implant is characterized by allowing the performance of the implant to be evaluated during its lifetime. Several variables such as temperature and forces [26–29], or more recently its stability are taken into account in this evaluation (Figure 1.3).
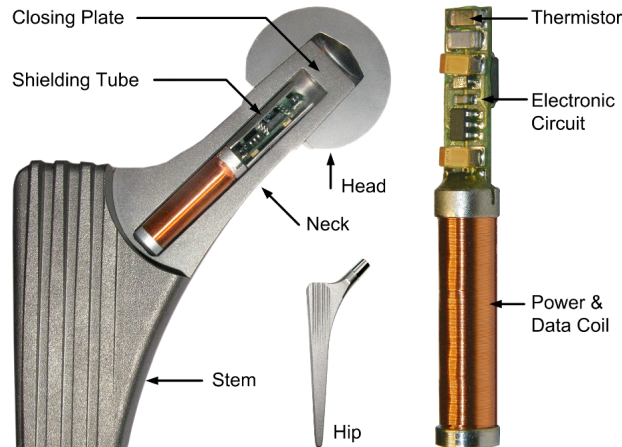


Figure 1.3: Illustration of an instrumented implant with the electronic system housed in the implant's head and neck. From Bergmann *et al.* [26].

**Instrumented active implants**

An instrumented active implant has the same monitoring ability as instrumented passive implant but it is able to stimulate bone growth simultaneously. This type of implants were proposed by Soares dos Santos *et al.* [30], who defends that this type of implant must fulfill five requirements: (i) monitoring systems providing data related to bone-implant fixation states; (ii) real-time processing systems to assess potential failure; (iii) actuation systems, to provide the delivery of personalized therapies when loosened regions are detected; (iv) telemetry system for external communication; (v) self-powering systems to electrically supply sensors, actuators and communication systems, while preserving an autonomous operation. With the development of this type of implants, the possibility to provide personalized therapies is foreseen by simulating target peri-implant regions.

## 1.5   Objectives

Extending the work previously developed by the research team from the Centre for Mechanical Technology and Automation (TEMA - University of Aveiro) focused on the design of smart implants, the main goal of this work is to create a prototype that allows the sensing of fixation states of bone implants. This goal requires:

- Development of a network of capacitive elements along a planar architecture that enable to monitor capacitance changes for different bone-implant bonding states;

- Development of a system for data acquisition and processing;

- Development of a website to control and monitor the data acquisition system, that allows the viewing of the data in a three dimensional graph;

- *In situ* experiment to analyse the performance of the prototype with bone structures to detect the capacitance variation.

The impossibility of performing the *in situ* test and the development of a real prototype, led to the alteration of the objectives of this work. So, following the same purpose the new requirement for achieving this goal are the following:

- Development of a system that simulates the data acquisition system;

- Development of a website to control and monitor the data acquisition system, that allows to view the data in a three dimensional graph;

- Development of the project for the prototype indicating all materials that are required and how to connect them.

# Chapter 2

# Literature Review

## 2.1 Bone properties

Bone is a strong and rigid connective tissue. It provides support and protection for the body and has the necessary rigidity to prevent the wearing of articular surfaces when under load. A high cell density enables it to change according to mechanical demands. The human body has different bones, in a total of 206, which vary in shape and in minor surface details. Many bones articulate with their neighbours at synovial joints. Regarding the microstructure of the bone, it contains specialized cells (osteoblasts, osteocytes and osteoclasts) surrounded by a mineralized collagenous extracellular matrix. The structure of the bone is formed by an organic matrix (30-40%) and minerals (60-70%). The organic matrix is formed by water (10-20%), collagen, proteins, glycoproteins and carbohydrates [31]. The inorganic part is formed by mineral salts ($Ca_{10}$ , $(PO_4)_6$). The ageing and metabolic factors alter this proportion. One example is the increase of the mineralization over the years.

### 2.1.1 Macroscopic structural classification

Bone macroscopic classification distinguishes cortical bone and trabecular bone (Figure 2.1). Cortical bone is compact and it provides resistance to bending and torsion due to these characteristics: it is the external layer of a bone and has a lower remodelling process per year, as well as it is a dense and solid mass. Trabecular bone, also called cancellous or spongy bone, exists in a large proportion inside the end of long bones and it accounts for 20% of the total skeleton mass [32].

### 2.1.2 Microscopic structural classification

There are two kinds of bone that can be identified on a microscopic level: woven and lamellar. Woven bone does not have a regular arrange of the collagen fibres and crystals and it is formed by a high concentration of osteoblasts during development. Lamellar bone is more organized and has a slower remodelling rate. In central regions of cortical bone, lamellae are organized in concentric cylinders. While lamellar bone makes up almost all of an adult skeleton, woven bone is typical in young fetal bones but is visible in adults during the bone remodelling process.
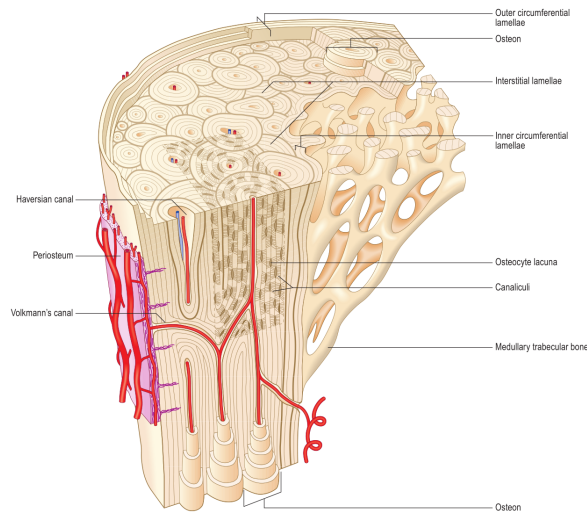
Figure 2.1: The main features of the microstructure of mature lamellar bone. Areas of compact and trabecular (cancellous) bone are included. Note the general construction of the osteons; distribution of the osteocyte lacunae; Haversian canals and their contents; resorption spaces; and different views of the structural basis of bone lamellation [31].

### 2.1.3   Bone cells

Osteoblasts, osteoclasts and osteocytes are the three categories of specialized bone cells which perform different functions during their lifetime. Osteoblasts are visible in the surface of bone being responsible for the secretion of collagen and the organic matrix of the bone. Once completely involved by bone matrix they became osteocytes. Osteoclasts dissolve the mineral part of the bone. They can be formed by the fusion of two or more cells, so they can have two or more nuclei. Osteocytes are distributed in the calcified bone matrix and they are interconnected by dendritic process [31].

### 2.1.4   Bone modelling and remodelling

Due to the constant use and friction between bones, they are in permanent remodelling and modelling. Modelling is the process which changes the size and form of the bone. Materials, including bones, are vulnerable to microdamage during repeated loading. In order to reduce the fatigue failure, old bone is replaced by new tissue, in a process called remodelling. New tissue does not need to have the same orientation as the old one. This process begins with resorption to remove the old bone and is followed by new bone formation being more frequent in trabecular bone. With the ageing, people decrease their activity and this and other metabolic factors cause bone loss. Thus, remodelling decreases with age. This process needs perfect coordination between osteoblasts and osteoclasts. Diseases such as OA and osteopetrosis are linked to the poor balance between the bone cells' activity [31, 33].

### 2.1.5  Mechanical Properties

As said before, bone has the potential to adapt according to different stimuli. Cortical bone has different properties in different directions, tensile/compressive moduli along longitudinal direction is higher than in radial or circumferential direction, and the strength is higher under compression in the longitudinal direction and lower under tensile loading in the transverse direction [34]. After reaching the yield point, mechanical properties modify and deterioration of tissue microstructure occurs. This process is known as microdamage. During the fatigue failure test, this bone has better results (higher resistance) in compression than in tension.

Mechanical properties of trabecular bone are determined by its highly porous material. The strength of trabecular bone is also higher in compression than in tension. When compressed above yield point, loss of stiffness and strength can occur and accumulative deformations could lead to clinical fractures. The ageing also affects the behaviour of trabecular bone, specially in density and architecture, which causes modulus and strength decrease.

### 2.1.6  Electrical Properties

Dielectric properties of bones tissues can be analysed on a molecular level, as the interaction between electrical radiation and cells [35]. The electrical behaviour of tissues vary with frequency. The dielectric spectrum of a tissue is characterized by three main relaxation regions $\alpha$, $\beta$ and $\gamma$ at low, medium and high frequencies [36]. These relaxation regions can be seen as a polarization mechanism. For a first order approximation the complex relative permittivity, $\hat{\varepsilon}$, is defined by a single time constant, $\tau$ and angular velocity $\omega$ as shown in equation 2.1.

$\varepsilon_{\infty}$ is the permittivity at frequencies where $\omega\tau \gg 1$ and $\varepsilon_s$ the permittivity at $\omega\tau \ll 1$.

$$\hat{\varepsilon} = \varepsilon_{\infty} + \frac{\varepsilon_s - \varepsilon_{\infty}}{1 + \jmath\omega\tau} \tag{2.1}$$

The complexity of the tissue's structure and composition resulted in an enrichment of the dispersion. Equation 2.2 is described in terms of multiple Cole-Cole dispersion which can predict dielectric behaviour with a correct choice of parameters. The new terms in this equation represent: permittivity in vacuum, $\varepsilon_0$, the conductivity, $\sigma_\imath$ and a parameter to measure the broadening of the dispersion, $\alpha$, known as distribution parameter.

$$\hat{\varepsilon}(\omega) = \varepsilon_{\infty} + \sum_n \frac{\Delta\varepsilon_n}{1 + (\jmath\omega\tau_n)^{(1-\alpha_n)}} + \frac{\sigma_\imath}{\jmath\varepsilon_0} \tag{2.2}$$

## 2.2  Monitoring of loosening states of bone implants

The monitoring of loosening states of the bone-implant interface can be carried out by different methodologies. Post-operative stability is measured in terms of migration and micromotion. Migration is the irreversible movement of the implant. Micromotion are the relative movements between the bone and the implant [37]. In this section, several

monitoring methods for cementless implants are analysed and identified by the technology input/output as in a previous work carried out by João Cachão *et al.* [38].

### 2.2.1   The image approach to monitor implant loosening states

Medical imaging used to assess the state of implants can be divided into invasive and non-invasive methods. An invasive method is characterized by the injection of an external agent in the body.

X-ray is a widely used non-invasive diagnosis method due to its low cost. This method provides bi-dimensional images of the body. It is considered a low resolution method for displacements less than 0.7 mm and aseptic loosening is only detectable when it is greater than 2 mm [39, 40]. Computed Tomography (CT), a non-invasive diagnosis method, is a diagnosis method which uses different x-ray images, in different angles, in order to have a three-dimensional image of the body [41] (Figure 2.2). Two other types of CT but as an invasive methods, which injects radioisotopes into the patients' body, are Positron Emission Tomography (PET) and Single Photon Emission Computed Tomography (SPECT).

MRI, a non-invasive diagnosis method, uses magnetic fields to generate images of the body. This method has good results for early states of loosening after a THA [42]. In recent years, scintigraphies (diagnosis methods that require the injection of radioactive substances to reconstruct images of the human body) have started to be used. The created images allow to identify the areas where there is a greater bone cell activity. The sensitivity of this method reached a value of 76% for aseptic loosening detection in 46 patients [43].
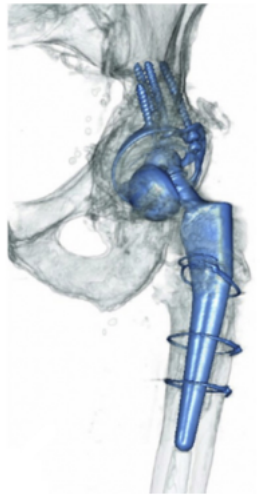


Figure 2.2: CT scan of a hip implant [41].

### Limitations of image monitoring technologies

Diagnostic imaging methods have some limitations. X-rays do not allow an exact quantification of the displacement of the implant and are also unable to provide data related to both micro-scale and large scale loosening. The newer methods, despite being

more accurate, are more expensive and also require the injection of an external agent. A general limitation to all these methods is the impossibility to monitor the bone-implant fixation states throughout the daily lives of patients, as monitoring operations must be performed in medical laboratories.

### 2.2.2   The vibrometric approach to monitor implant loosening states

The analysis of implant fixation state in relation to the bones can be evaluated based on vibrometric methods. This type of methods has been studied intensively in recent years, presenting better results than the methods based on medical images [44].

The methods already proposed require the application of excitations in the tissues surrounding the bone-implant interface and monitoring with a technology that can be embedded in the implant or extracorporeal.

Concerning **extracorporeal mechanical excitations (input) and extracorporeal mechanical signal (output)** it is possible to distinguish seven technologies. The generic representation of this methodology is presented in Figure 2.3.

Georgiou *et al.* [44], using a shaker and an accelerometer in the knee and the hip, respectively, proved that the presence of harmonics was an indicator of implant loosening. This stability was only studied for hip implants and two states can be detected: secure or loss.

Alshuhri *et al.* [45,46], with a shaker (femoral lateral condyle) and two accelerometers (iliac crest and greater trochanter) detected acetabular cup loosening through the analysis of harmonic ratios. Two loosening states were detected.

Rieger *et al.* [47], using a shaker (knee) and three accelerometers (medial condyle, iliac crest and greater trochanter), identified frequency shifts as a measure to detect failed implant integration of total hip replacement. Two states were detected: secure or loose.

After few years, Rieger *et al.* [48] developed a technology to detect loosening of hip endoprostheses using piezoelectric actuators arranged on a spherical cap to drive shock waves. As in the previous work, frequency shifts were used to detect the two levels of integration (secure or loose).

Lannoca *et al.* [49] and Varini *et al.* [50], using a piezoelectric actuator and an accelerometer, measured the stability of an implant by the detection of shifts in the resonance frequency. Stable and quasi-stable implants were distinguished. In the same studies, these authors tested the use of a displacement transducer (LVDT), in order to measure micromotions in the primary stability of the implant. Different micromotions correspond to different stabilities.

Pastrav *et al.* [51], with a shaker and a mechanical impedance head, also identified frequency shifts as a measure to detect different stages of insertion, allowing a good initial fixation.

Jiang, Lee and Yuan [52] used an isokinetic dynamometer (based on knee motions) and an accelerometer (patella), in order to analyse the spectral power ratios of dominant poles. This study distinguished secure and loose implants.
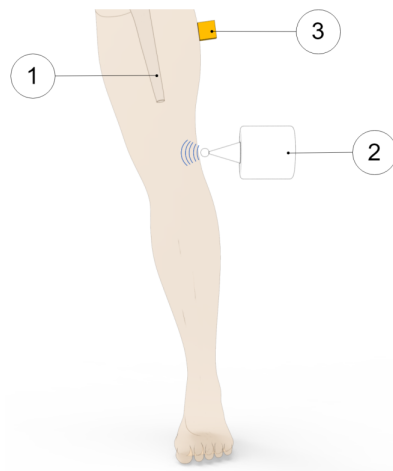
Figure 2.3: Illustration of extracorporeal mechanical excitation (input)/extracorporeal mechanical signal (output) for vibrometric fixations: (1) implant, (2) vibrator providing the input excitation, and (3) extracorporeal accelerometer measuring the resulting vibration from the implant–bone system. Figure depicting a hip implant case [38].

Concerning **extracorporeal magnetic induction (input) and extracorporeal mechanical signal (output)**, Ruther *et al.* [53,54] used small magnetic spheres attached to a flat spring inside the implant to produce oscillations of the bone-implant system and detect loosening. A magnetic field caused the collision between the oscillators and the implant. These collisions caused wave propagation which can be measured by an accelerometer. With the measurement of these waves, it is possible to analyse frequency shifts and the central frequency and associate these variables with different levels of loosening: secure, slight loss, significant loss. The experimental apparatus is illustrated in Figure 2.4.
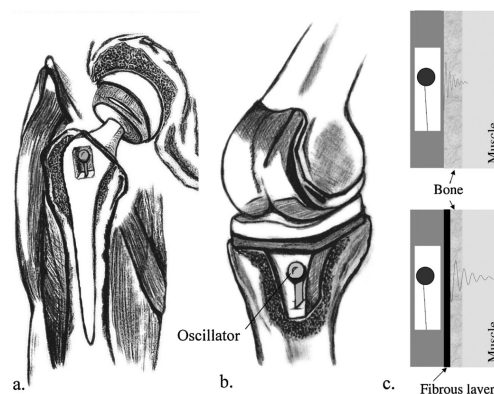


Figure 2.4: Endoprosthetic implants with integrated oscillator. (a) Total hip replacement. (b) Total knee replacement. (c) Section of the oscillator-implant system [53].

Concerning **intracorporeal mechanical excitation (input) and extracorporeal mechanical signal (output)**, only one technology was proposed by Glaser *et al.* [55]. Using two accelerometers (greater trochanter and anterior superior iliac spine) to detect the frequency amplitude of the impact made by the femoral head and acetabular component, different loosening states were measured.

### Limitations of vibrometric monitoring technologies

On the first method (extracorporeal mechanical excitations and extracorporeal mechanical signal) only the last two technologies were studied *in vivo* and the remaining were studied *in vitro*. Related to the periodicity of evaluation, [49], [50], [51] restricted it to an intra-operatively test and the others are restricted to the laboratory. On the second one, only *in vitro* tests were performed and is restricted to a laboratory environment. On the last method, although it was studied *in vivo*, it is also restricted to a laboratory.

It is important to highlight the huge influence that the surrounding tissues have on the wave propagation using the vibrometric methods. The use of extracorporeal components can be uncomfortable for the patient and limit the use of these methods during the daily life. Almost all methods distinguish solely two states: loss or secure, being strongly influenced by the implant material, once the latter will influence the wave propagation.

### 2.2.3   The acoustic approach to monitor implant loosening states

Acoustic Emission (AE) is the phenomenon of sonic and ultrasonic wave generation by materials as they undergo deformation and fracture processes [56]. Different methods based on this acoustic emission were studied in order to monitor implant loosening states.

Concerning **extracorporeal mechanical excitation (input) and extracorporeal acoustic signal (output)** it is possible to distinguish three technologies.

Unger *et al.* [57] developed a monitoring system with extracorporeal excitation (metallic object hitting the implant) that produces sound and uses an extracorporeal microphone (lateral condyle) to monitor the produced sound. Implant loosening can be detected by the resonance frequency, which increases with the stability. Damped output was also observed with an increase of stability.

Alshuhri *et al.* [45, 46] used the same apparatus described for the vibrometric approach (both approaches are represented in Figure 2.5), the only difference is the use of an ultrasound probe replacing the accelerometer. Loosening states are detected in the same manner but higher harmonic ratios are detected with an acoustic approach. Two loosening states were observed.

Goossens *et al.* [58], using a hammer to drive excitation to the system and a microphone to capture the output signal, detected different states of hip implants. This states were identified by shifts in the resonance frequency.
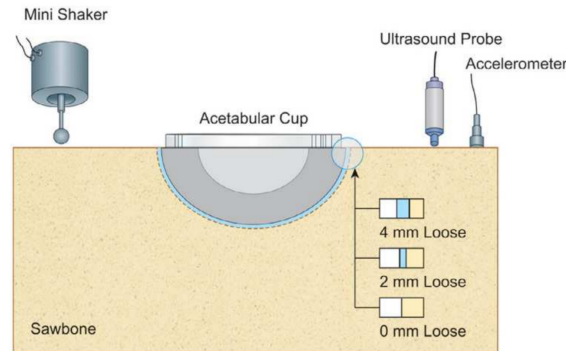
Figure 2.5: Vibrometric and acoustic approaches, proposed by Alshuhri *et al.*, illustrating the excitation (mini-shaker) and measurement methods (ultrasound probe and accelerometer) [45].

Concerning **intracorporeal mechanical excitation (input) and extracorporeal acoustic signal (output)**, a single technology was implemented by Glaser *et al.* [55, 59]. This study was based on the vibrometric approach developed by the same authors but with the use of a sound transducer instead of accelerometers, allowing the analysis of acoustic emissions. Loosening states were distinguished in the same manner (high frequency and amplitude), with both methodologies demonstrating a high correlation level.

Concerning **extracorporeal magnetic induction (input) and extracorporeal acoustic signal (output)**, only one method was proposed by Ewald *et al.* [60,61], with a similar apparatus used in the vibrometric approach by Ruther *et al.* [53, 54]. Using a microphone to record the output signal, it was possible to associate different fixation states with shifts in the resonance frequency measured using the microphone.

### Limitations of acoustic monitoring technologies

Analysing the validation tests, only the methodology proposed by Glaser *et al.* was performed *in vivo*, in 29 patients. The remaining investigation teams performed diverse *in vitro* tests.

Contrarily to the vibrometric approach, none of these methodologies is performed intra-operatively, but they are all limited to the laboratory environment, compromising the daily monitoring of the patient.

As in the vibrometric approach, the acoustic approach is influenced by the tissues surrounding the implant. The results of the acoustic approaches can be influenced by external noises to the loosening detection mechanism. The use of hammers to cause mechanical excitation can cause pain to the patient. The use of magnetic induction as excitation can be seen as an attempt to minimize the patients discomfort. It is also important to highlight that, although different loosening states can be identified, the regions where loosening occurs can not be identified by any proposed technology.

### 2.2.4 The bioelectric impedance approach to monitor implant loosening states

Different biological tissues have different dielectric properties, so it is possible to identify different tissues through electrical bioimpedance. Considering this fact, Arpaia *et al.* [62, 63] proposed a method with **extracorporeal electrical current (input) and extracorporeal electric potential difference (output)**. In this method, a current is delivered at the skin and the voltage drop is measured between two electrodes. The impedance between the electrodes can be used to identify different loosening states. An increase in the impedance is related to a superior loosening level.
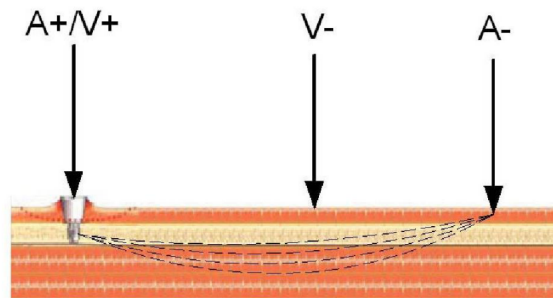


Figure 2.6: Schematic of the bioelectric impedance approach. The A+/A- represents the alternate current and the V- is the voltage drop [63].

### Limitations of bioelectric impedance monitoring technologies

As it is necessary to measure the impedance, this test is limited to laboratory environment. This technology was tested *in vivo* and *in vitro*. As on the previous approach, the region where the loosening occurs can not be identified. Due to the variation on the patient's tissue, it is difficult to define a standard metric.

### 2.2.5 The magnetic induction approach to monitor implant loosening states

Concerning **extracorporeal magnetic induction (input) and extracorporeal magnetic induction (output)**, two different studies were developed.

Ewald *et al.* [60] incorporated a piezo crystal within the implant that is later activated by a coil. An extracorporeal coil is used to measure the vibrations generated. The measurement of the amplitude of the output signal, generated through constant frequencies, can be used to measure the fixation states.

Ruther *et al.* [64] used a similar technology to the one in their vibrometric work but altered the method of detecting the output signal. In this approach, the output signal is detected by an extracorporeal coil that measures the velocity of the oscillation caused by the impact. By measuring the velocity, it is possible to identify the state of the bone-implant fixation.

**Limitations of magnetic induction monitoring technologies**

The proposed technologies were analysed in a laboratory environment and were only validated *in vitro*. The fact that instrumentation is used extracorporeally, these methods become unable to monitor the patients' routine. The detection performed by these methods is also located in a specific area of the prosthesis. To allow the collection of data along the overall region, the number of components used would have to be increased. Finally, it should be stressed that the use of non-magnetic materials in the implant interfaces is fundamental to enable the use of the magnetic induction phenomenon.

### 2.2.6   The strain approach to monitor implant loosening states

Bone deformations can be measured with extensometers that allow the evaluation of bone deformation. For measurements on the human body, the use of extensometers is restricted due to biocompatibility factors which emerge by bonding them to bone structures.

Two different methods were developed in order to study this approach. The first was developed by Burton *et al.* [65] who used a methodology based on **intracorporeal mechanical loads (input) and intracorporeal bone deformation (output)**. A sensor with two cosurface circuits was developed and it allowed the measurement of axial and radial strain. These circuits are connected to a capacitor whose dieletric changes as the strain changes. Shifts in resonance frequency allow the evaluation of different loosening states. Figure 2.7 illustrates this approach.
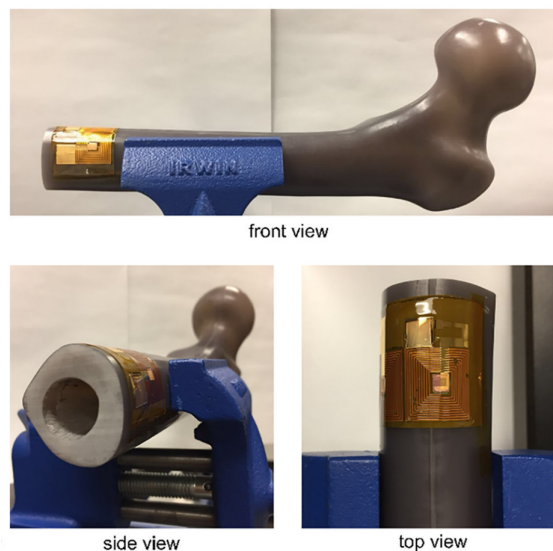


Figure 2.7: Application of the strain approach developed by Burton *et al*, where the strain sensor is visible [65].

The other technology is based on **intracorporeal mechanical loads (input) and intracorporeal fixation plate deformation (output)**. McGilvray *et al.* [66] developed a microelectromechanical system to assess the bone fixation state. This device comprises planar capacitors and a resonance circuit and it is powered by an

extracorporeal antenna which emits an eletromagnetic wave and receives the sensor's signal. Changes in capacitance are found as shifts in the resonance frequency, which in turn are related to fracture healing state.

### Limitations of strain monitoring technologies

Both methodologies were studied *in vitro* but the last one was also study *in vivo*. In the first method, the need to contact the bone may change the bone-implant physiological state and, consequently, the bone-implant fixation. For the second method, the fact that it requires the evaluation of the frequency of resonance by magnetic induction requires a laboratory environment to minimize noise interference.

### 2.2.7   The capacitive approach to monitor implant loosening states

Luís Henriques [67] investigated an unique method with **intracorporeal voltage excitation (input) and intracorporeal electric capacitance (output)**. By using planar electrodes, it was possible to measure variations in electrical capacitance during different bone-implant bonding states. This study proved the possibility of monitoring the bone implant interface from planar capacitive systems. It was equally possible to observe that increases in the electrical capacitance occur by decreasing the bone-sensor distance.

### 2.2.8   Monitoring technologies for instrumented implants

The following technologies were already proposed and used in instrumented implants using a cemented fixation, although it is possible to use them in cementless implants.

Various authors explored the possibility of developing systems with **extracorporeal mechanical excitation (input) and intracorporeal mechanical signal (output)**. Puers *et al.* [68] developed an instrumented hip prothesis which uses some electronics and accelerometers. Two different fixation states can be detected (secure or loose) by analysing the waveform distortion of the output signal (Figure 2.8).

Marschner *et al.* [69] measured shifts in the resonance frequency using a two-axis accelerometer, some eletronics and a shaker in order to detect two loosening states (proximally loose and proximally secure). This implant also has the ability to perform wireless monitoring and is inductively powered.

Sauer *et al.* [70] followed a similar approach as Marschner [69] but using a three axis acceleration sensor and a shaker (central part of the femur). The loosening states can be distinguished as maximum, medium and minimum, by analysing shifts in resonance frequency.
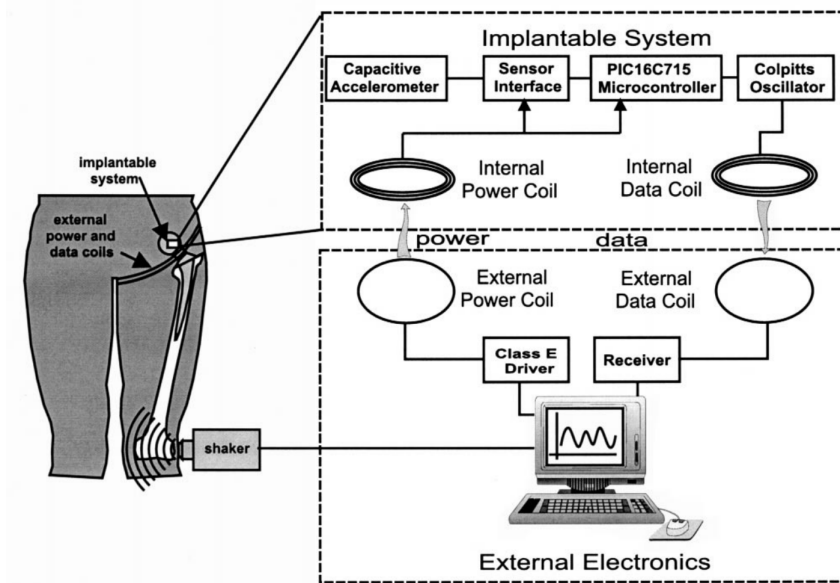
Figure 2.8: System, developed by Puers *et al.* [68] for the detection of hip prosthesis loosening.


**Limitations**

These three monitoring systems can only operate *in vitro* and are restricted to laboratory environment. Instrumented implants were developed to incorporate some electronics, but data processing continues to be done extracorporeally. The development of advanced sensing systems for incorporation within the implants is harder to achieve, and their effectiveness is reduced compared to cosurface capacitance systems.

# Chapter 3

# Materials and Methods

To enable the monitoring of bone-implant fixation states, an architecture is proposed to allow the data acquisition of data from a network of planar capacitors printed in inner regions near the surface of instrumented bone implants. Figure 3.1 aims to represent the overall system view of the proposed architecture.

The system consists on a data acquisition part and a monitoring/control interface. The data acquisition system is composed by a Raspberry Pi, a capacitance-to-digital converter (EVAL AD-7746) and the sensing system that will incorporate the implants comprising the network of capacitance sensors. The monitoring system consists of a website controlled by the clinician who will follow up the performance of the implants.
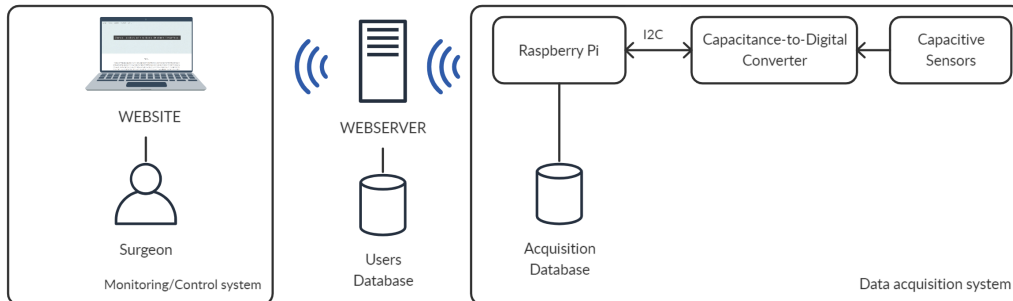


Figure 3.1: Overall system structure.

Given the impossibility of implementing the overall prototype, the work was focused on the development of the monitoring/control system and the Raspberry Pi was used to simulate the data acquisition system.

## 3.1 Sensing technology

Capacitive sensing technologies have the ability of detecting changes in its surroundings induced by variations in the dielectric. These variations can be observed as a change in the sensor's capacitance. These systems are characterized by low energy consumption, reduced manufacturing cost and the possibility of being miniaturized. In the previous work using this technology, only one capacitor was used [67]. To validate that with a more significant number of capacitors, it is possible to monitor the bone-implant

fixation states in several regions, a Printed Circuit Board (PCB) was designed using the software EAGLE (v9.5.2,Autodesk). This board contains a total of twelve capacitors (with interdigitated architectures) arranged in a 4x3 matrix with the following characteristics: (i) 2.5 mm spacing between rows; (ii) 4 mm spacing between columns; (iii) 0.5 mm gap between electrodes; (iv) a total footprint dimension of each capacitor of 7.5x7.5 mm (Figure 3.2).
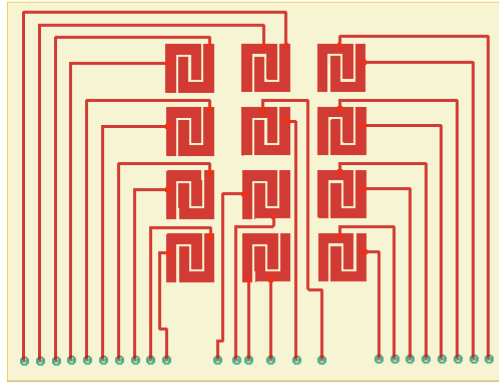


Figure 3.2: Schematic from Eagle 9.5.2 software.

## 3.2   Raspberry Pi 4

The use of this device instead of others, like a LattePanda, is due to the fact that the Raspberry Pi allows an $I^2C$ communication with a direct configuration in Python, which is important for the real experimental apparatus. This device is used to generate data and save it in the correct database.

The micro SD card used has Debian 10.3 installed. To become easier to develop code inside the Raspberry Pi, CODE-OSS 1.14 was also used. Other essential step was to turn the Raspberry into a web server with the installation of Apache, PHP interpreter and MySQL server. These softwares facilitate the manages of databases and the communication between the computer where the website is host.



Figure 3.3: Raspberry Pi 4. (from *www.raspberrypi.org*)

## 3.3 Databases

### 3.3.1 Database host in main webserver

For an easier management/storage of data it was created a database called **users**, which has several tables as presented in Figure 3.4. The first table that was created is the table **login**, which includes the variables defined when an account is created. These variables do not change during the implant lifetime except the column **time_sampling**, that can be altered. Each username has a specific table, with the same name as the username. Each row of this table represents a patient and has the variables used to monitor and control the data acquisition system. Both tables can be read and updated by the Raspberry Pi.

| users **login** |
| --- |
| id: int(11) |
| username: varchar(255) |
| password: varchar(255) |
| patient_name: varchar(255) |
| prosthesis_name: varchar(255) |
| time_sampling: int(11) |
| no_capacitors: int(11) |
| numMed: int(11) |
| ip: char(15) |

| users **ines** |
| --- |
| id: int(11) |
| patient_name: varchar(255) |
| no_capacitors: int(11) |
| day: int(11) |
| now: int(11) |
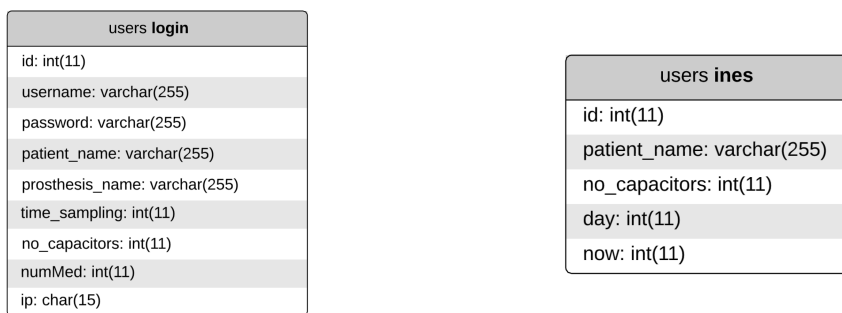
Figure 3.4: Users Database.

### 3.3.2 Database host in Raspberry Pi 4

The first step to configure the data acquisition system is to create a database named with the patient name where the implant is inserted. This database has one fixed table named **graph** (Figure 3.5 on the left). The **x** column represents the x position of the center of each capacitor; the **y** column has the same purpose but in the Y axis, **z** column is the bone-sensor distance measured, and **capacitance** is the capacitance measured by the capacitor in the bone surroundings. There were also created so many tables in the database as the number of capacitors incorporated within the instrumented implants. These tables are named **capacitorX**, where X is a number higher or equal to 1 up to the number of planar capacitors of the network. Capacitor 1 is illustrated in the Figure 3.5 on the right.

| maria **graph** |
| --- |
| id: int(11) |
| date_hour: timestamp |
| x: float |
| y: float |
| z: float |
| capacitance: float |

| maria **capacitor1** |
| --- |
| id: int(11) |
| displacement: float |

Figure 3.5: Patient Database.

## 3.4   Software Development

The need to assess the bone-implant fixation state constitutes a significant step before proceeding with revision surgery. In this regard, a web application was developed to allow the connection between the clinician and the data acquisition system incorporated within the instrumented implants. For the development of the website, it is necessary to use a server. Initially, the Apache II server was used. However, the need to have a Python interpreter for the elaboration of various graphs and the reduced dimension of the application, led to the change in the use of Apache II for Django. Thus, the web application was developed with Django which is a high-level Python Web framework [71].

### 3.4.1   Home Page

This is the page that is loaded when the website is accessed, and is constituted by different sections: (i) About section (Figures B.1 and B.2); (ii) Create section (Figure B.3); (iii) Contact section (Figure B.4). Some parts of the design were based on W3SCHOOL functions and the About section was written based on literature review.

**'Create' Form**

The 'create' form (Figure 3.6) is the first form that appears on the website. This form must be submitted in two different situations: (i) the clinician wants to create an account; (ii) the clinician wants to include a new patient in an existing account.



Figure 3.6: 'Create' form.

This form has a total of eight variables that must be inserted. The **Username** and the **Password** are the identifiers for the login and allow to control the data acquisition system during the lifetime of the implants. **Patient**, must be filled with the patients' name and surname, separated by an underscore, in order to prevent mistakes in the case of multiple patients with the same first name. **No Acquis**, represents the total number of acquisitions that the sensing technology must do before converting the mean value into a bone-implant distance. **Capacitor Type** can be filled with a, b or c depending on the capacitive architecture. The **No. Capacitors** must be a multiple of three, once they are arranged in 3 columns and the capacitors are added in full rows. **Time Sampling** represent the interval between acquisition measured in days. **IP Identifier** is the IP of the Raspberry Pi that is connected to the data acquisition system. Figure 3.7 describes the activity flow of this form. At the same time that the login page is displayed all the variables are saved in the users database.
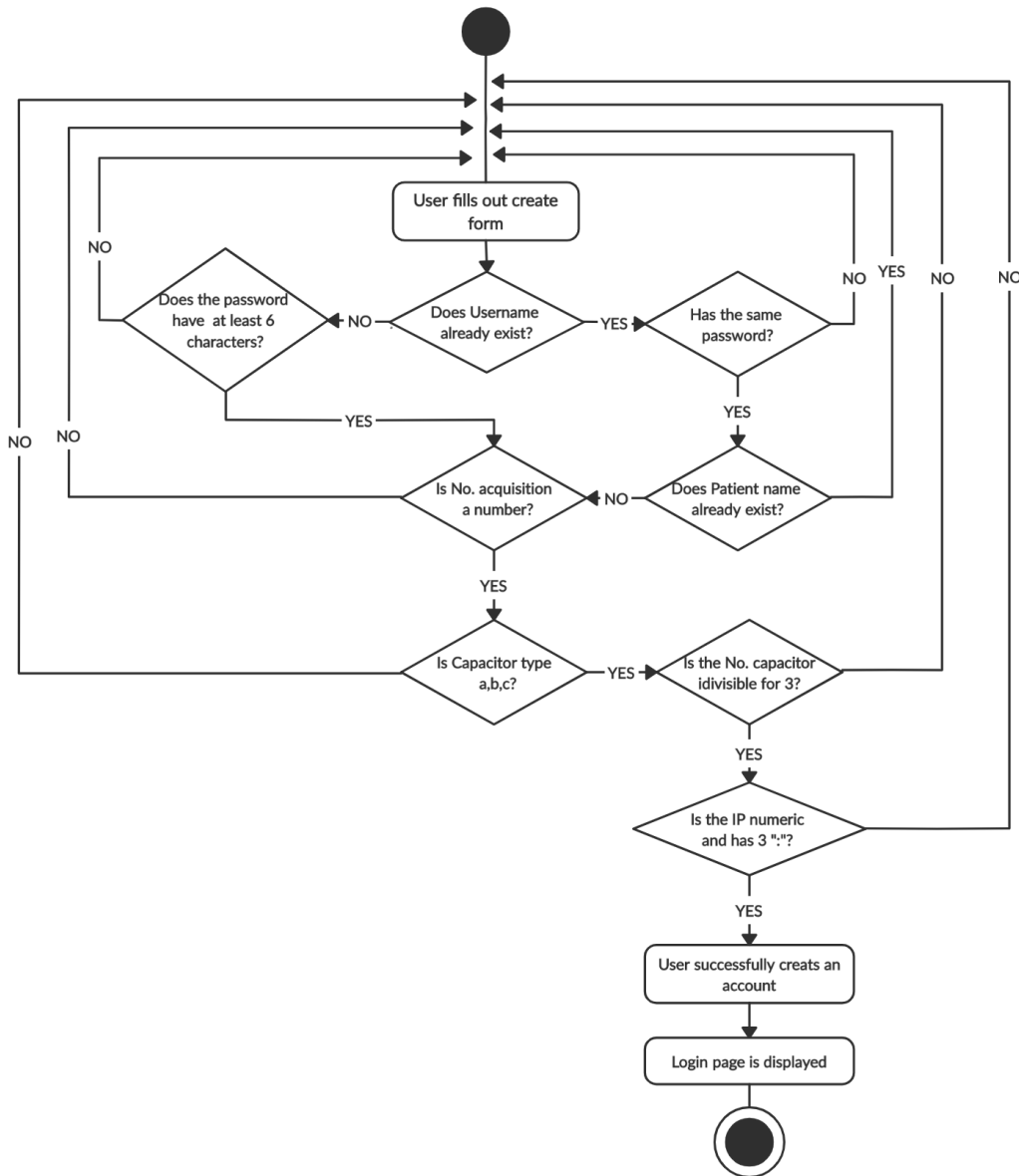
Figure 3.7: Activity UML for the 'create' form.

**'Contact' Form**

During the use of this application some doubts might arise. This section (Figure 3.8) was developed to facilitate the communication between the clinician and the research team.

Once the form is submitted, the research team will receive the message such that technical support can be provided. If the user did not introduce a valid email, it will be impossible to answer. Figure 3.9 on the left describes the activity flow of this form. The function *send_mail* from DJANGO was used.

Figure 3.8: 'Contact' form.

### 3.4.2   Login Page

This page (Figure B.5) appears after the creation of a new account or, if the clinician already has an account, it can be easily accessed through the navigation bar. This form will appear and it must be filled with the credentials that were defined when the account was created, like an usual login page. Figure 3.9 on the right, describes the activity flow of this form. To explain the interactions between the different objects, Figure 3.10 illustrates the UML sequence for this form.
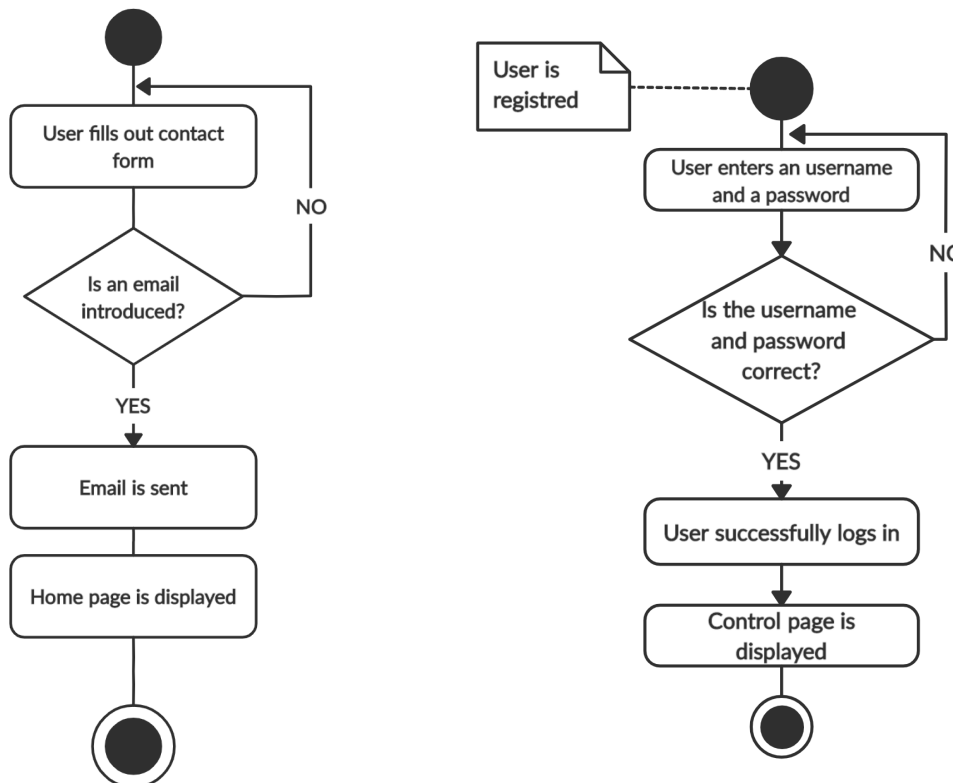


Figure 3.9: UML activity for the 'contact' form (left) and 'login' form (right).
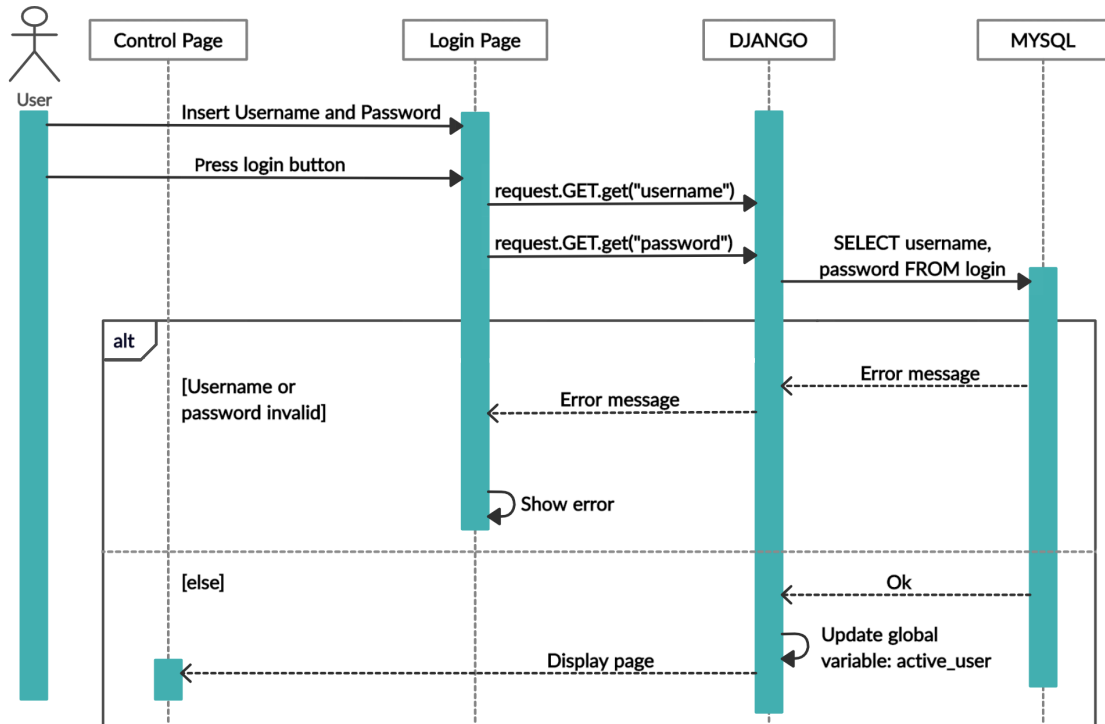
Figure 3.10: UML sequence for 'login' form.

### 3.4.3 Control Page

This page (Figure B.6) allows the data monitoring and data visualization of data from the data acquisition system using different methods. The **patient** name (Figure 3.11 on the left) must be the first variable to insert on this page. Skipping this step may result in getting data that do not match the patient in analysis, since this step makes the connection to the right data acquisition system.



Figure 3.11: Form to introduce the patient name, which is aimed to be analysed, and form to update the Time Sampling.

Although **Time Sampling** was defined when the user created the account, this value can be changed during the patients' life using the corresponding form (Figure 3.11 on the right). In order to explain the interactions that occur after the both forms are filled, Figure 3.12 and 3.13 show the UML sequence of each form.
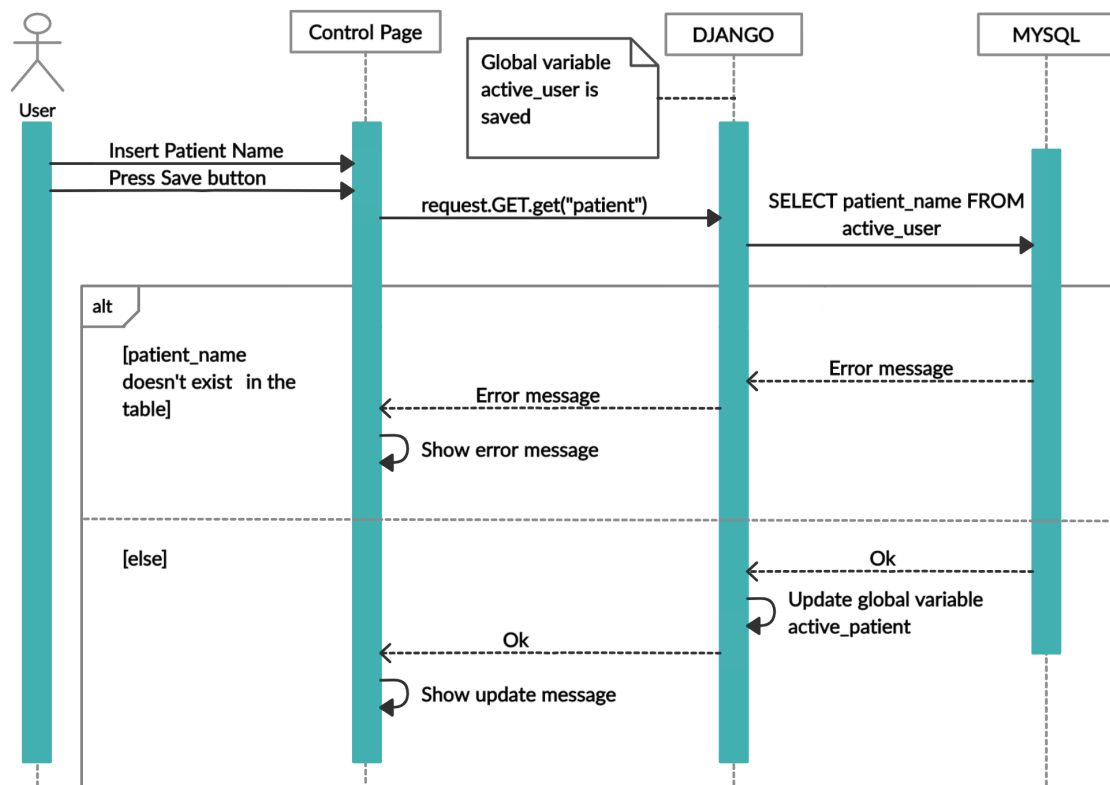
Figure 3.12: UML sequence to update patient record.
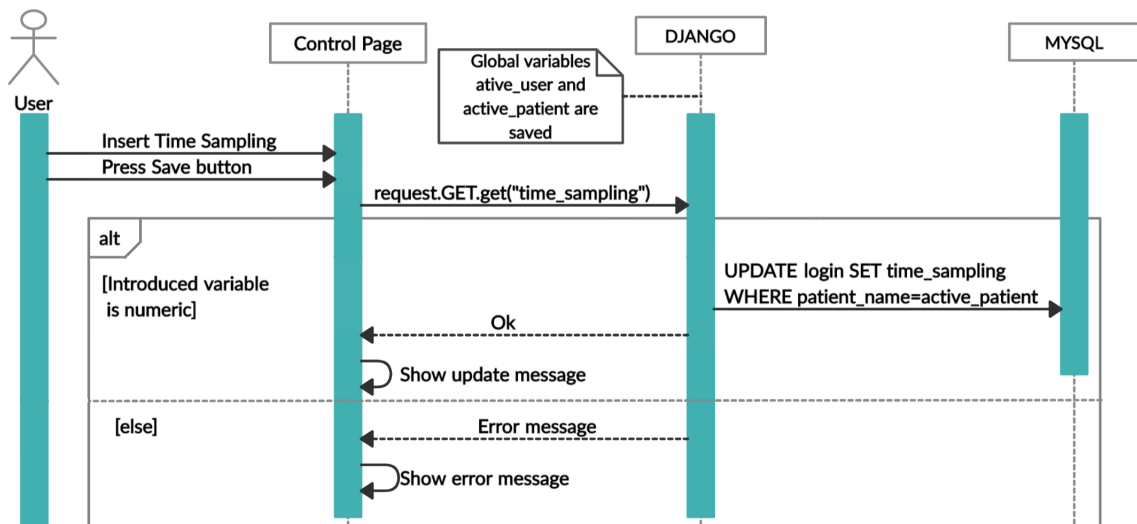


Figure 3.13: UML sequence to update the Time Sampling.

To evaluate the bone-implant fixation, it is possible to analyse two different graphs. The first is a three dimensional representation of the bone on a specific **Day** that the

user must indicate in the form (Figure 3.14 on the left) considering that the day 1 is the day of the primary surgery. In the three dimensional plot, the $x$ and $y$ axis correspond to the position of the capacitors and the $z$ axis corresponds the bone-sensor distance (in mm).



Figure 3.14: Form to introduce the day to analyse in a three dimensional plot and form to analyse a specific region throughout different days.

For a more detailed analysis of a specific region of the bone-implant interface, in which each region is related with each capacitor, a two dimensional plot can be visualized after the form **No. Capacitor** is filled (Figure 3.14 on the right). In the two dimensional plot, the $x$ axis represents the time when the data were acquired and the $y$ axis is the bone-implant distance (in mm). The Figure 3.15, describes the activity flow for visualization of the two plots (the three dimensional plot is described in the left). On the other hand, Figure 3.16 and Figure 3.17 shows the UML sequence for the respective forms.
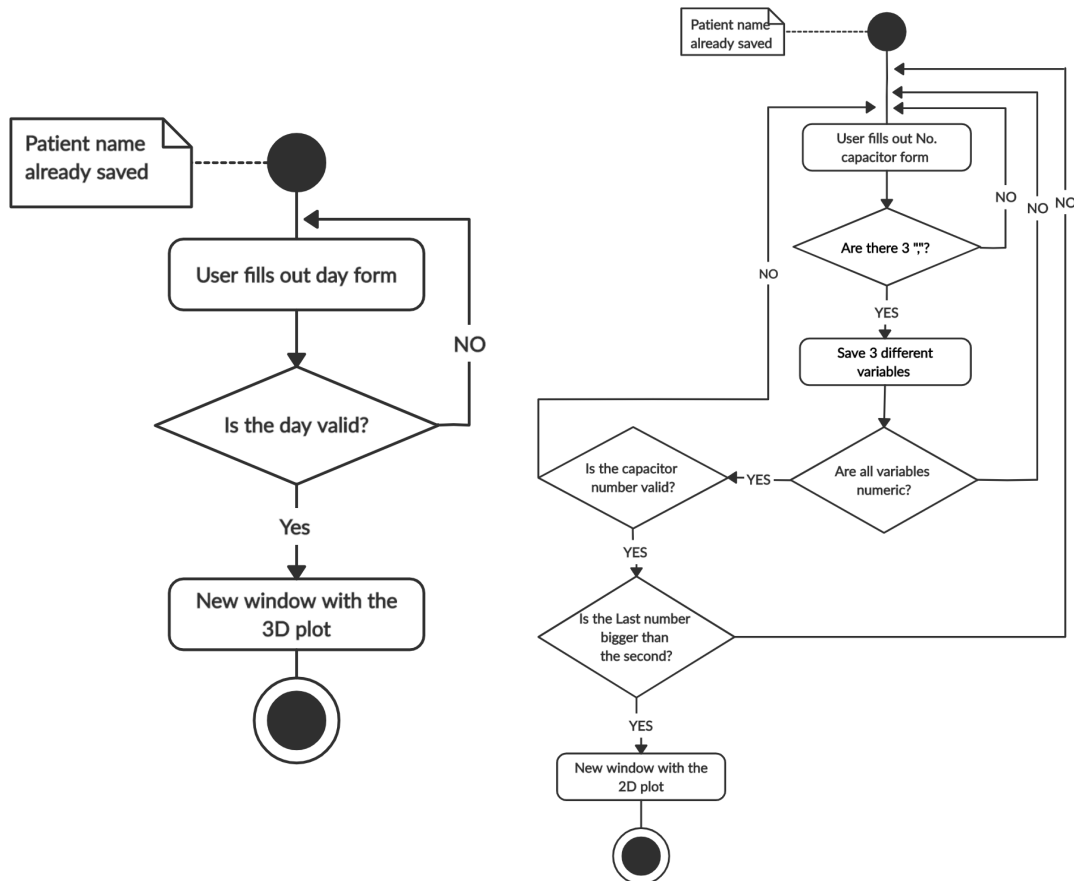


Figure 3.15: UML activity for three dimensional plot (left) and two dimensional plot (right).
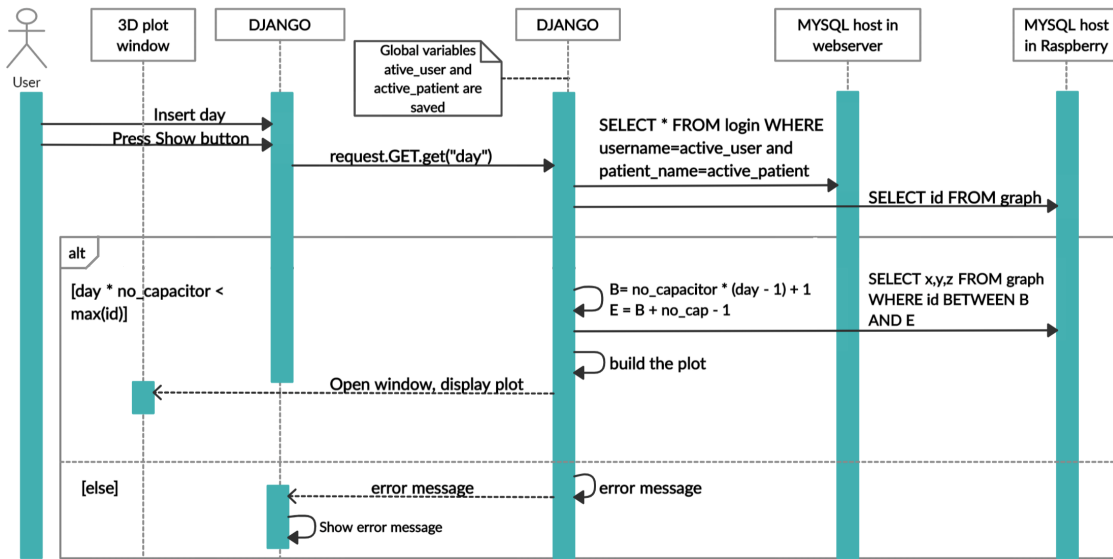
Figure 3.16: UML sequence to display the three dimensional plot.
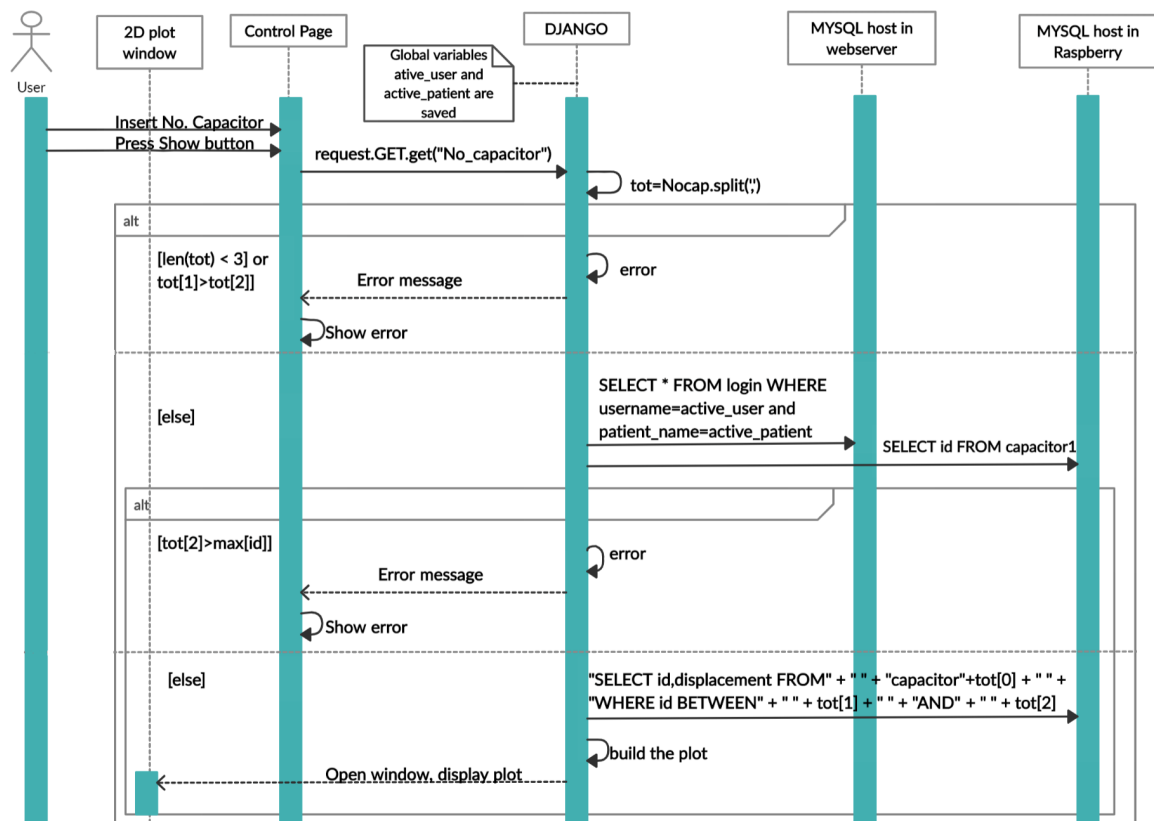


Figure 3.17: UML sequence to display the two dimensional plot.

During a medical appointment, by clicking on the button **Now** (Figure 3.18 left) it is possible to get the current data into a three dimensional graph with identical characteristics of the **Day** plot; this can be useful for an analysis of a specific movement of the joint. The UML sequence that defines the interactions between the user and the data acquisition system is illustrated in Figure 3.19.



Figure 3.18: Buttons to do an actual acquisition and the download.
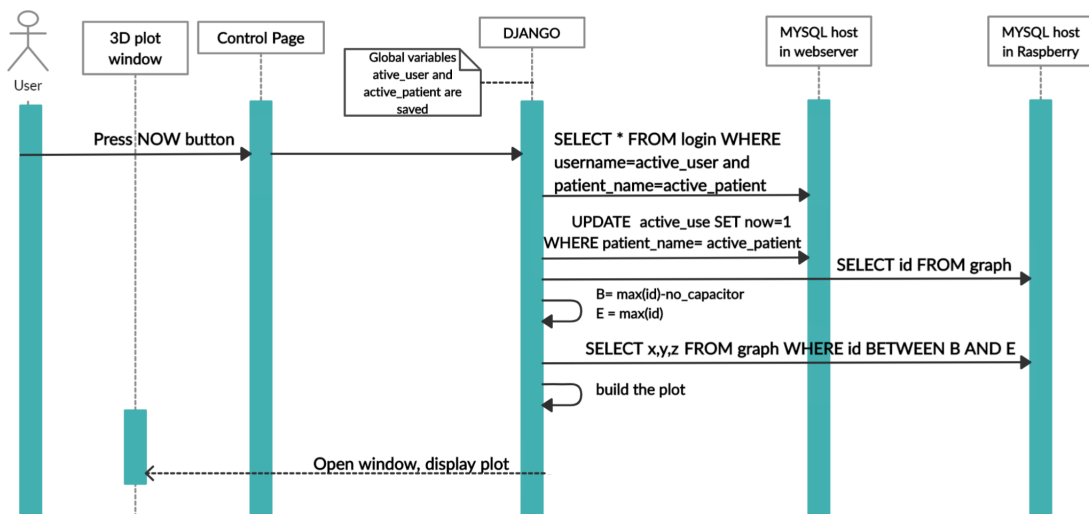


Figure 3.19: UML sequence to plot the actual displacement values.

The clinician may also need to perform an independent analysis of the data acquired from the implant. Thus, it is possible to download such data to an Excel file, by clicking the **Download** button (Figure 3.18 right), which comprises a table with all the data acquired from the patient in analysis. Each row has the time of the acquisition, the $x$ and $y$ position of the capacitor, the bone-sensor distance, and the measured capacitance. Figure 3.20 illustrates UML sequence to download the Excel file.
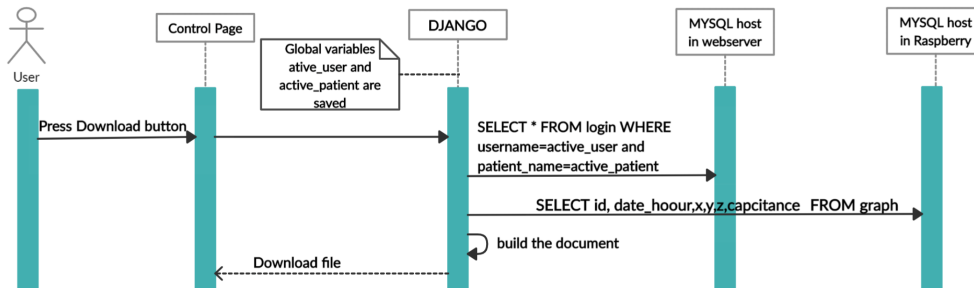
Figure 3.20: Sequence UML to download the Excel file.

## 3.5   Validation tests

### 3.5.1   Random Values Test

After the first connection to the database host in the main webserver, the Raspberry Pi can read and update different values. Note that in both tables it is only possible to perform these operations if the **patient_name** corresponds to the patient where the implant is inserted.

With this step, the number of capacitors, time sampling and the remaining variables became information saved in Raspberry Pi. The number of capacitors divided by three represent the number of rows of the matrix of capacitors. With this number it is possible to know in which position (x,y) the center of each capacitor is.

In a previous work developed by Rodrigo Bernardo [72], it was defined a six-order polynomial that allows to calculate the capacitance based on the distance between the bone and the capacitor.
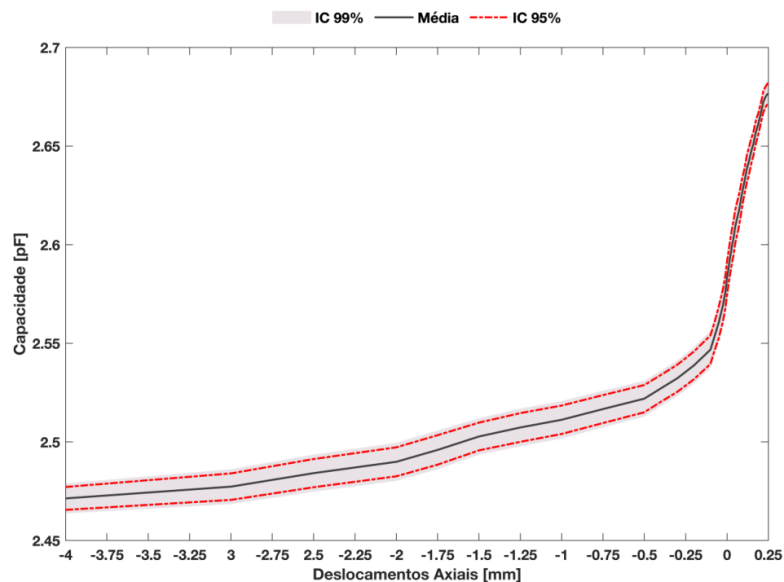


Figure 3.21:   Average capacitance for porcine samples in an approximation and compression scenario [72].

$$C(x) = \sum_{i=0}^{6} p_i x^i; \quad -4 \leq x \leq 0.25 \quad [mm] \tag{3.1}$$

$p_0 = 2,588$, $p_1 = 0,2925$, $p_2 = 0,4217$, $p_3 = 0,2894$, $p_4 = 0,09628$, $p_5 = 0,01495$, $p_6 = 0,0008502$

This polynomial was obtained through multiple capacitance measurements for various distance positions from the bone to the capacitive sensing technology, during a compression test. Figure 3.22 on the left, illustrates the various positions that were considered in this test. A simplified scheme of the experimental apparatus for this *in vitro* test is illustrated in Figure 3.22 on the right. The used bone sampling has a geometry of 10x10x10 mm and the contact between the capacitor and the bone is made through a 1 mm thick polimeric layer.
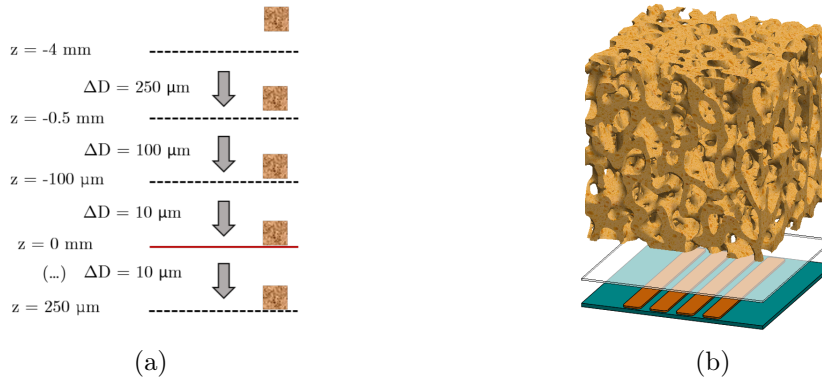


Figure 3.22: Schematic of the compression test and bone-sensor interface during the experimental test that led to obtain the six-order polynomial: a) Scheme illustrating the compression test. b) Scheme of the sensing interface used in compression test. [67]

To compute the bone-implant distance it was created a table with all bone-implant distances and the related measured capacitance (in the range between -4 mm and 0.25 mm). Having a capacitance value, it is possible to perform a linear regression between the two closest values in order to find the distance value. This approximation is valid once there are slight variations of capacitance/distance in near regions and the polynomial has a good correlation coefficient.

With this table it became possible to calculate the distance following the present steps:

- Calculate a random number between 2.4649 pF and 2.6924 pF;

- Calculate a number 5% greater and other 5% less than the calculated in the previous point;

- Generate **numMed** (this value is introduced by the website user) random values which must be contained in the interval calculated before and compute the mean of these values;

- Find the position in the table, and based on the previous and the next value of capacitance, compute the distance.

Note that the second step is performed since, in a real experimental test, more than one acquisition of data is performed for the same bone position. So in order to approach this test to the real one, there is a need to reduce the interval for the generation of new values made in the third step.

Now that the position (x,y) of the capacitor, the capacitance and related bone-sensor distance are known, it is possible to insert these values into the different tables of the database executing two different queries, one for the graph table and other which will be executed as many times as the number of capacitors, to insert a new row in each table capacitorX.

The position $(x,y)$ of the capacitor remains constant during the implant lifetime, which does not happen with the capacitance and consequently the distance. Thus, the previous steps are repeated with the periodicity indicated in the time sampling (measured in days).

This code is also in a function which runs every second in order to evaluate if the 'now' button is pressed. If this occurs, a new value of distance is computed at the moment and inserted in the database.

### 3.5.2 Simulation of an approximation test

In order to simulate an approximation test, a bone sample with different heights was defined (Figure 3.23). The polynomial described by equation 3.1 only evaluates distances from a distance of 4 mm to contact. For this reason, a distance of 4 mm was considered the initial position of the sample to the capacitor.
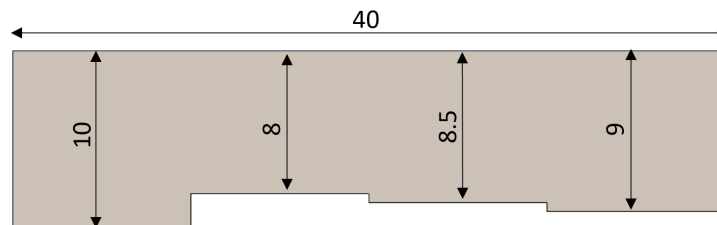


Figure 3.23: Schematics of the bone sample.

Subsequently, distances of 0.25 mm were defined until there was contact between the capacitor and the region of bone that has a higher height (Figure 3.24 left). After the contact, it was also simulated that there was a bone regeneration until all the different parts of the sample contact with the capacitor (Figure 3.24 right). The values were also obtained based on the table created for the previous test.
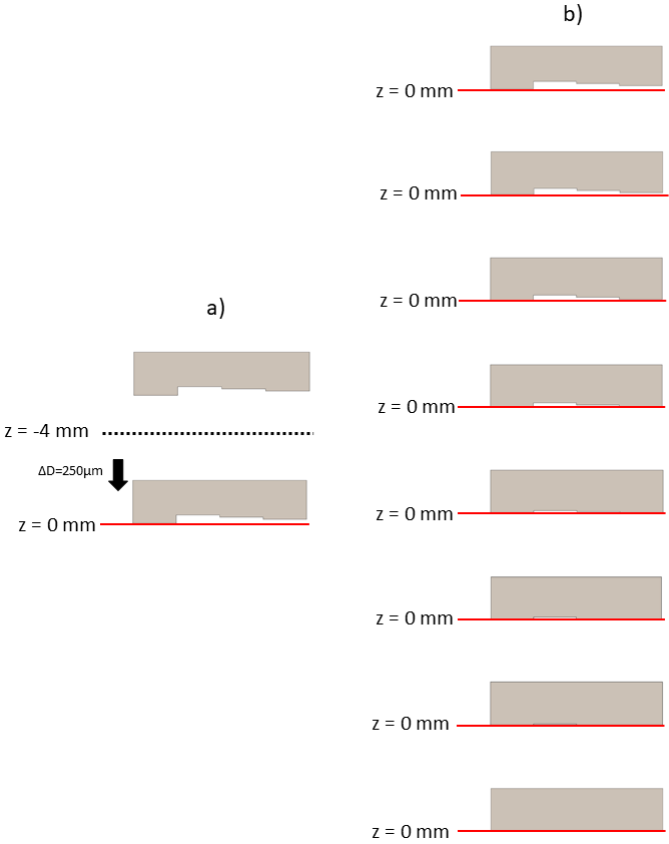
Figure 3.24: Scheme illustrating the compression and regeneration test: a) compression b) regeneration.

# Chapter 4

# Results

This chapter aims to present the results obtained after two simulation tests. The analysis started with the creation of an account on the website. Later, the control page was accessed to visualize the bone-implant fixations state according to the proposed methods.

## 4.1  Random values test

In order to verify the operation of this application, a user named "ines" was created with the patient name "maria_peres". The remaining variables inserted are shown in the Figure 4.1.



| Username | ines | | Capacitor Type | a |
| Password | •••••• | | No. Capacitors | 12 |
| Patient | maria_peres | | Time Sampling | 5 |
| No Acquis. | 20 | | IP identifier | 192.168.1.12 |

Create

Figure 4.1: Submitted form.

As shown in the Figure 4.1, the time sampling is 5, so every 5 days a new acquisition of capacitance is conducted and converted into a distance. However, in order to reduce the acquisition time, a day is simulated as a minute in this test, so each 5 minutes a new value is computed.

Data were acquired and saved in the respective database. During this time, the control page was accessed several times and the data were analysed by different methods. In the following figures, different plots are shown. Each one corresponds to a different day of acquisition. As it can be seen, the values do not present a realistic evolution of the state of the bone-implant status, as they were randomly acquired. With a real experiment test machine, the values will present realistic bone-implant distances for different regions.

Note that the value of 0 in the $z$ axis is represented in the bottom to simulate where the capacitor is positioned. The negative values present the position of the bone relative to the capacitor.



(a) First acquisition

(b) Tenth acquisition

(c) Twenty-third acquisition

(d) Sixtieth acquisition
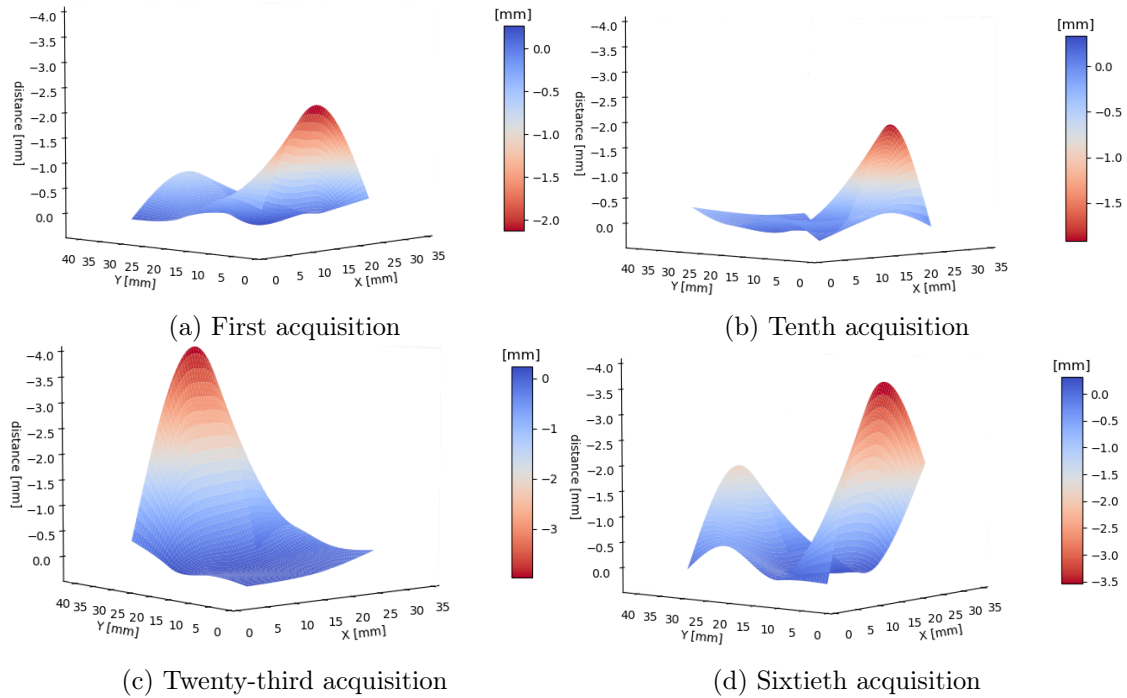
Figure 4.2: Three dimensional plot for different days of the random validation test.

As explained in the previous chapter, data can be analysed in different regions (where each region is related with each capacitor) over time. The numbering of each capacitor started in the first row and first column and increases by column and later by row (Figure 4.3).



Figure 4.3: Schematic with the numbering of the network of capacitor printed in the PCB.

The two dimensional plots present the distance ($y$ axis) between the chosen days ($x$ axis). The following figures illustrate the distance in all capacitors between the first day and the sixtieth day. Once again, these plots only demonstrate that it is possible to acquire data from different parts of the implant.
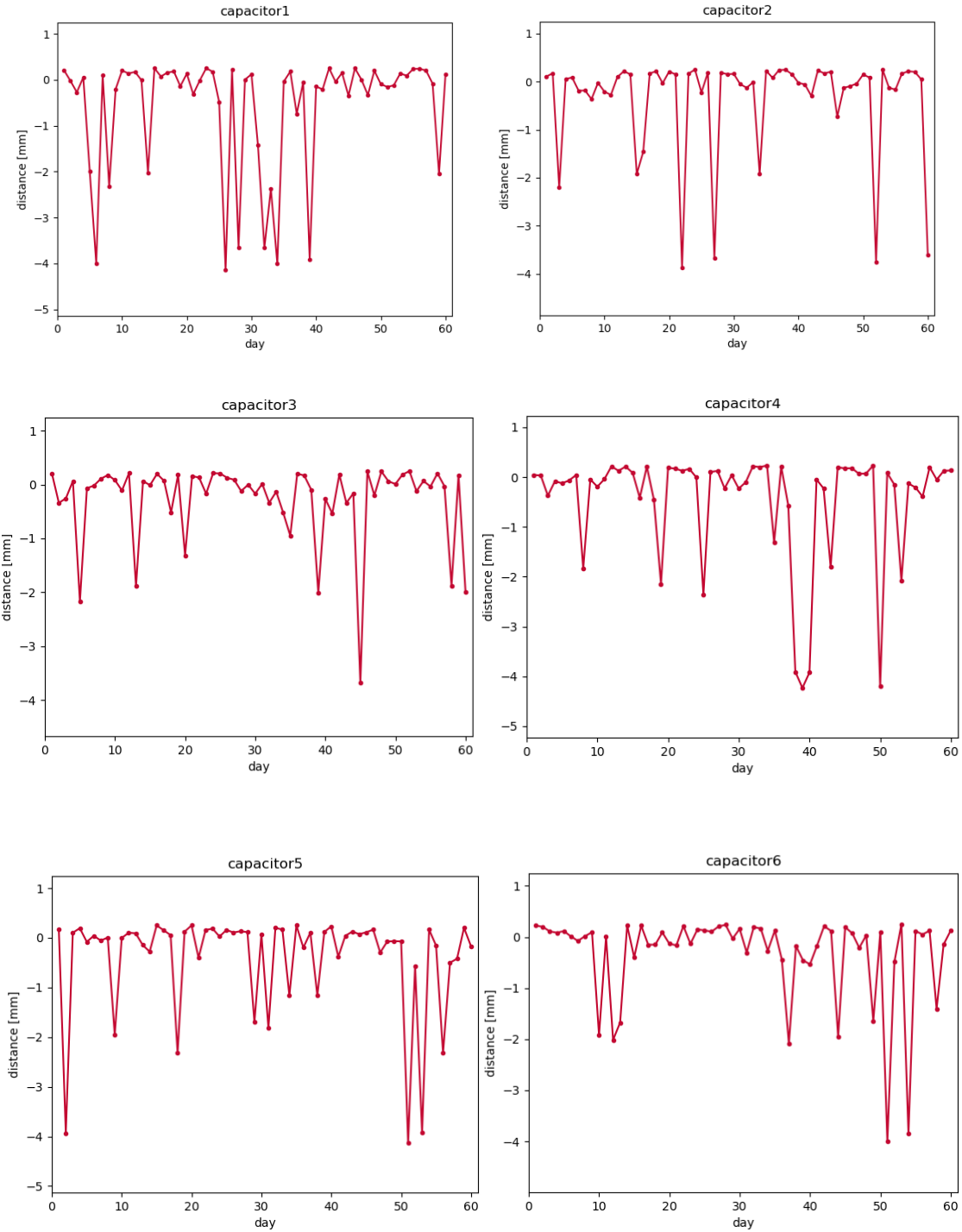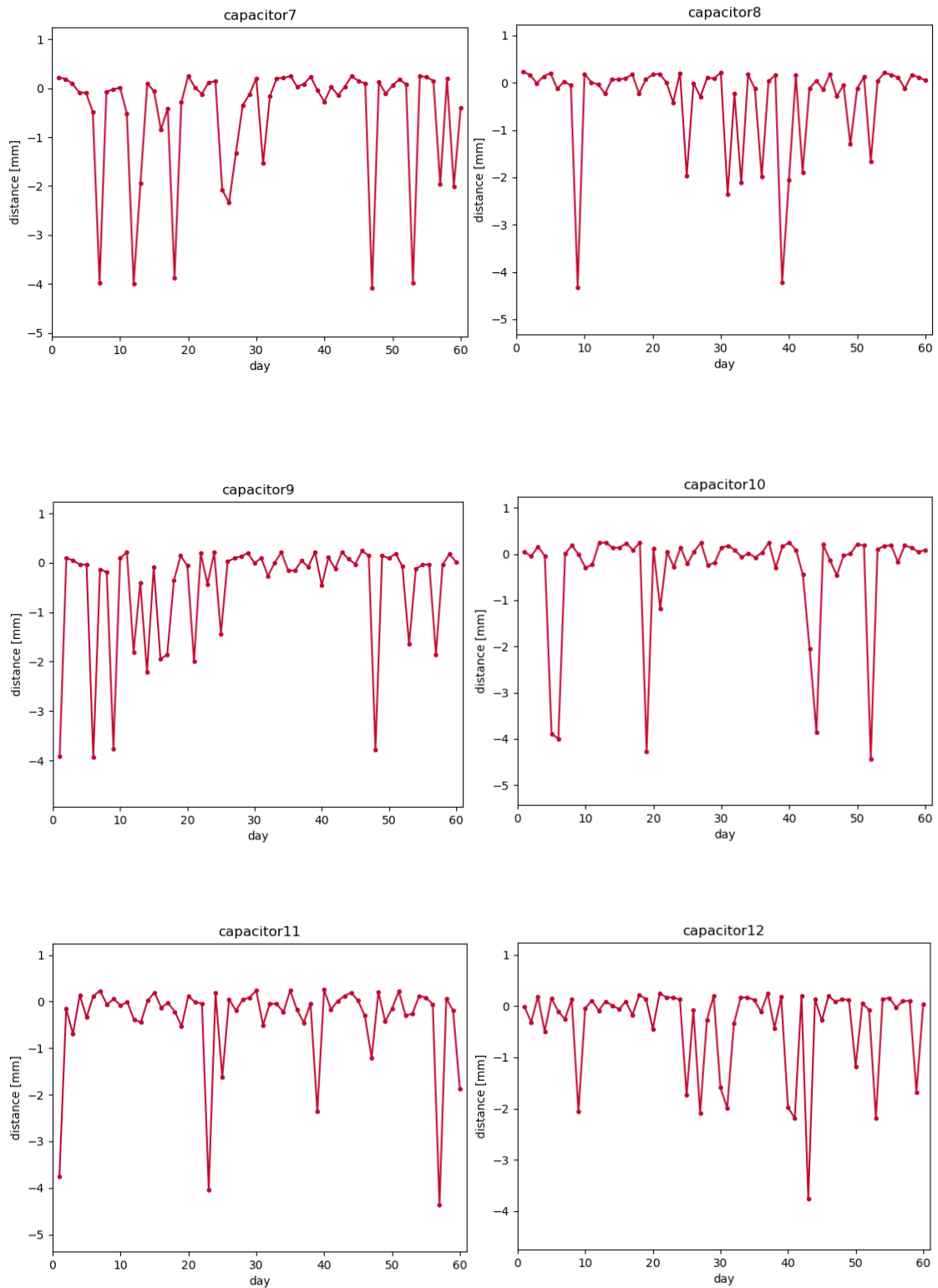
Figure 4.4: Data acquired in each capacitor between the first and the sixtieth day.

The 'now' button allows to acquire data at the moment that it is pressed. After the data is acquired, a three dimensional plot is displayed. This button was also pressed during the simulation test and the result is presented in the following figure.
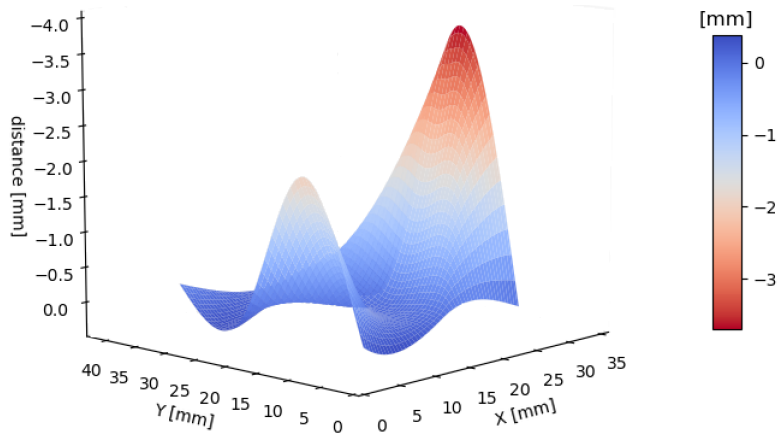


Figure 4.5: Data acquired after clicking on 'now' button.

## 4.2   Approximation test

To carry out this assessment, each displacement of 0.25 mm is performed every 5 minutes. So, nine acquisitions were carried out until the bonding of bone sample with the interfacial polymeric sheet occurs, and eight acquisitions until all samples are in the bonding scenario. The following figures present 6 out of the 17 acquisitions in the three dimensional plots.



(a) First acquisition

(b) Fifth acquisition

(a) Tenth acquisition

(b) Fifteenth acquisition

(c) Sixteenth acquisition

(d) Seventeenth acquisition
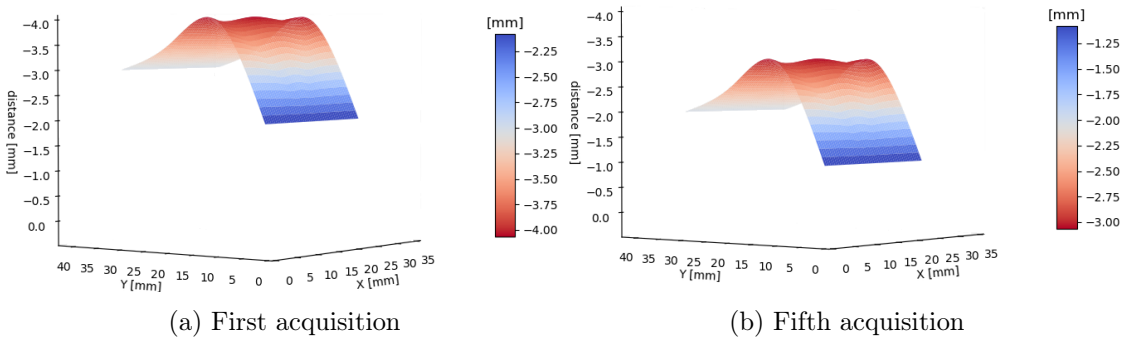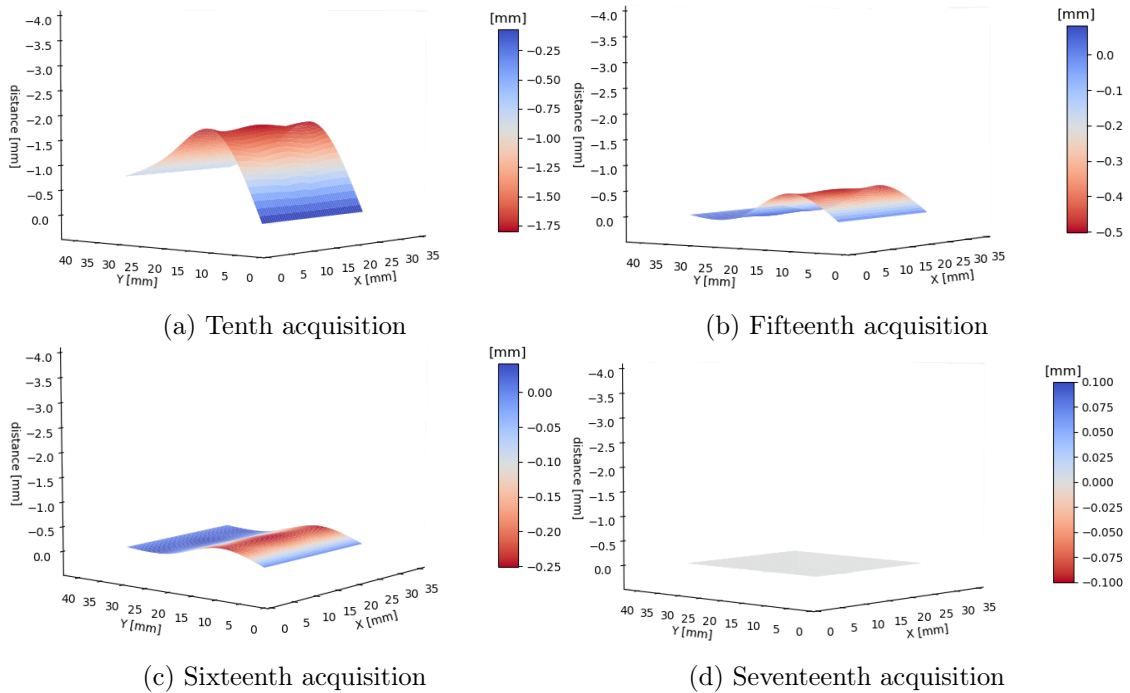
Figure 4.7: Three dimensional plots for different days of the approximation validation test.

In contrast to the previous results, it is possible to analyse the evolution of the bone towards the capacitor, placed in the position 0 of the $z$ axis. The similarity between this test and the real one shows that is possible to visualize minor variations of distance in a three dimensional plot.

The bone sample was designed in order to have the same height for each row of the capacitor matrix. So, the values acquired for each capacitor placed in the same row are the same. Taken this specification into consideration, the illustration of the two dimensional graphs (Figure 4.8) was only performed for one capacitor of each row.
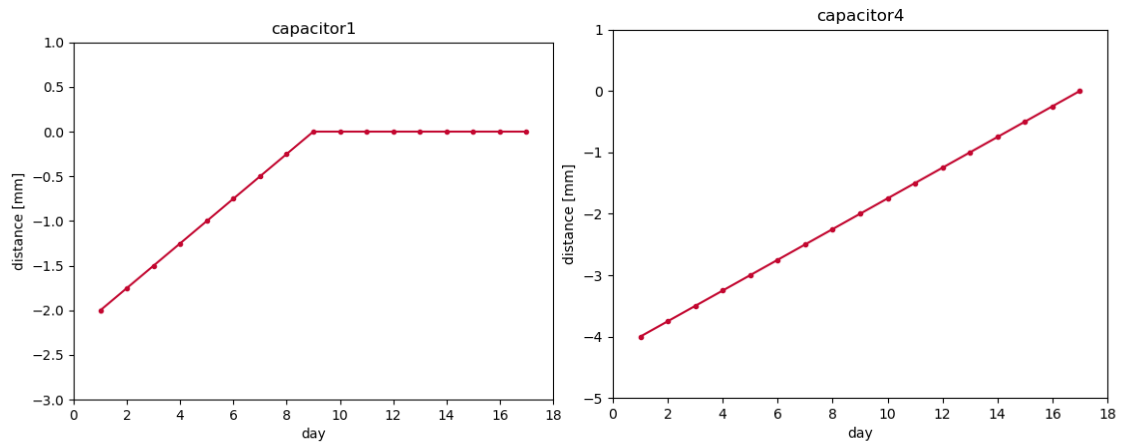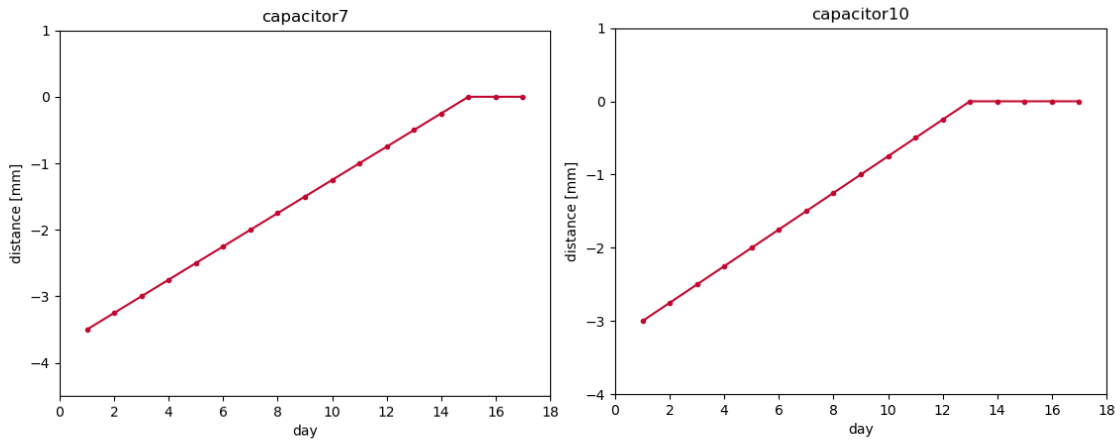
Figure 4.8: Data acquired in the first capacitor of each row between the approximation test.

The download button allows to save an Excel file on the computer. As shown in Table 4.1, it is possible to verify that the file has five columns: the time that the data is acquired, $x$ position of the capacitor, $y$ position of the capacitor, the distance and the capacitance.

Although not all values were presented in the two dimensional plots, they are saved within the Excel file with the same distance for each row of capacitors. After downloading the file, it was performed a modification in order to consider just the same acquisition as the represented in the three dimensional plots. The first acquisition is illustrated in yellow.

Table 4.1: Example of an Excel file downloaded to the PC.

| Date | X [mm] | Y [mm] | Distance [mm] | Capacitance [pF] |
|---|---|---|---|---|
| 16/06/20 18:18:37 | 7,5 | 7,5 | -2 | 2,491 |
| 16/06/20 18:18:37 | 19 | 7,5 | -2 | 2,491 |
| 16/06/20 18:18:37 | 30,5 | 7,5 | -2 | 2,491 |
| 16/06/20 18:18:37 | 7,5 | 17,5 | -4 | 2,465 |
| 16/06/20 18:18:37 | 19 | 17,5 | -4 | 2,465 |
| 16/06/20 18:18:37 | 30,5 | 17,5 | -4 | 2,465 |
| 16/06/20 18:18:37 | 7,5 | 27,5 | -3,5 | 2,481 |
| 16/06/20 18:18:37 | 19 | 27,5 | -3,5 | 2,481 |
| 16/06/20 18:18:37 | 30,5 | 27,5 | -3,5 | 2,481 |
| 16/06/20 18:18:37 | 7,5 | 37,5 | -3 | 2,481 |
| 16/06/20 18:18:37 | 19 | 37,5 | -3 | 2,481 |
| 16/06/20 18:18:37 | 30,5 | 37,5 | -3 | 2,481 |
| 16/06/20 18:38:37 | 7,5 | 7,5 | -1 | 2,510 |
| 16/06/20 18:38:37 | 19 | 7,5 | -1 | 2,510 |
| 16/06/20 18:38:37 | 30,5 | 7,5 | -1 | 2,510 |
| 16/06/20 18:38:37 | 7,5 | 17,5 | -3 | 2,481 |
| 16/06/20 18:38:37 | 19 | 17,5 | -3 | 2,481 |
| 16/06/20 18:38:37 | 30,5 | 17,5 | -3 | 2,481 |
| 16/06/20 18:38:37 | 7,5 | 27,5 | -2,5 | 2,481 |
| 16/06/20 18:38:37 | 19 | 27,5 | -2,5 | 2,481 |
| 16/06/20 18:38:37 | 30,5 | 27,5 | -2,5 | 2,481 |
| 16/06/20 18:38:37 | 7,5 | 37,5 | -2 | 2,491 |
| 16/06/20 18:38:37 | 19 | 37,5 | -2 | 2,491 |
| 16/06/20 18:38:37 | 30,5 | 37,5 | -2 | 2,491 |
| 16/06/20 19:03:38 | 7,5 | 7,5 | 0 | 2,588 |
| 16/06/20 19:03:38 | 19 | 7,5 | 0 | 2,588 |
| 16/06/20 19:03:38 | 30,5 | 7,5 | 0 | 2,588 |
| 16/06/20 19:03:38 | 7,5 | 17,5 | -1,75 | 2,499 |
| 16/06/20 19:03:38 | 19 | 17,5 | -1,75 | 2,499 |
| 16/06/20 19:03:38 | 30,5 | 17,5 | -1,75 | 2,499 |
| 16/06/20 19:03:38 | 7,5 | 27,5 | -1,25 | 2,509 |
| 16/06/20 19:03:38 | 19 | 27,5 | -1,25 | 2,509 |
| 16/06/20 19:03:38 | 30,5 | 27,5 | -1,25 | 2,509 |
| 16/06/20 19:03:38 | 7,5 | 37,5 | -0,75 | 2,511 |
| 16/06/20 19:03:38 | 19 | 37,5 | -0,75 | 2,511 |
| 16/06/20 19:03:38 | 30,5 | 37,5 | -0,75 | 2,511 |
| 16/06/20 19:28:38 | 7,5 | 7,5 | 0 | 2,588 |
| 16/06/20 19:28:38 | 19 | 7,5 | 0 | 2,588 |
| 16/06/20 19:28:38 | 30,5 | 7,5 | 0 | 2,588 |
| 16/06/20 19:28:38 | 7,5 | 17,5 | -0,5 | 2,517 |
| 16/06/20 19:28:38 | 19 | 17,5 | -0,5 | 2,517 |
| 16/06/20 19:28:38 | 30,5 | 17,5 | -0,5 | 2,517 |
| 16/06/20 19:28:38 | 7,5 | 27,5 | 0 | 2,588 |
| 16/06/20 19:28:38 | 19 | 27,5 | 0 | 2,588 |
| 16/06/20 19:28:38 | 30,5 | 27,5 | 0 | 2,588 |
| 16/06/20 19:28:38 | 7,5 | 37,5 | 0 | 2,588 |
| 16/06/20 19:28:38 | 19 | 37,5 | 0 | 2,588 |
| 16/06/20 19:28:38 | 30,5 | 37,5 | 0 | 2,588 |
| 16/06/20 19:33:38 | 7,5 | 7,5 | 0 | 2,588 |
| 16/06/20 19:33:38 | 19 | 7,5 | 0 | 2,588 |
| 16/06/20 19:33:38 | 30,5 | 7,5 | 0 | 2,588 |
| 16/06/20 19:33:38 | 7,5 | 17,5 | -0,25 | 2,537 |
| 16/06/20 19:33:38 | 19 | 17,5 | -0,25 | 2,537 |
| 16/06/20 19:33:38 | 30,5 | 17,5 | -0,25 | 2,537 |
| 16/06/20 19:33:38 | 7,5 | 27,5 | 0 | 2,588 |
| 16/06/20 19:33:38 | 19 | 27,5 | 0 | 2,588 |
| 16/06/20 19:33:38 | 30,5 | 27,5 | 0 | 2,588 |
| 16/06/20 19:33:38 | 7,5 | 37,5 | 0 | 2,588 |
| 16/06/20 19:33:38 | 19 | 37,5 | 0 | 2,588 |
| 16/06/20 19:33:38 | 30,5 | 37,5 | 0 | 2,588 |
| 16/06/20 19:38:38 | 7,5 | 7,5 | 0 | 2,588 |
| 16/06/20 19:38:38 | 19 | 7,5 | 0 | 2,588 |
| 16/06/20 19:38:38 | 30,5 | 7,5 | 0 | 2,588 |
| 16/06/20 19:38:38 | 7,5 | 17,5 | 0 | 2,588 |
| 16/06/20 19:38:38 | 19 | 17,5 | 0 | 2,588 |
| 16/06/20 19:38:38 | 30,5 | 17,5 | 0 | 2,588 |
| 16/06/20 19:38:38 | 7,5 | 27,5 | 0 | 2,588 |
| 16/06/20 19:38:38 | 19 | 27,5 | 0 | 2,588 |
| 16/06/20 19:38:38 | 30,5 | 27,5 | 0 | 2,588 |
| 16/06/20 19:38:38 | 7,5 | 37,5 | 0 | 2,588 |
| 16/06/20 19:38:38 | 19 | 37,5 | 0 | 2,588 |
| 16/06/20 19:38:38 | 30,5 | 37,5 | 0 | 2,588 |

# Chapter 5

# Project for the experimental apparatus

In order to be able to continue the work developed and allow a realistic test *in vitro* in a laboratory environment, the overall sensing system and experimental apparatus were engineered. In this regard, this chapter gives a description of all the materials/technologies that need to be developed and acquired to enable *in situ* and *in vitro* testing.

## 5.1 Sensing technology

As explained on section 3.1, the capacitive structures allow the detection of dielectric variations. For the experimental project, three different capacitors (Figure 5.1) were designed and disposed in different PCB. Each board contains a total of twelve capacitors (of the same type) arranged in a 4x3 matrix. In order to be able to produce a later analysis of the performance of each type of capacitor, some variables were kept constant: (i) 2.5 mm spacing between rows; (ii) 4 mm spacing between columns; (iii) 0.5 mm gap between electrodes; (iv) a total footprint dimension of each capacitor of 7.5x7.5 mm.



Figure 5.1: Schematic of the interdigitated, squared and striped architectures.

## 5.2   Data acquisition and processing

Data acquisition must be conducted by using an EVAL-AD7746 to obtain the capacitance values through I$^2$C communication. The following sections indicate the various materials required to implement the data acquisition system. Figure 5.2 shows how they are electrically connected.
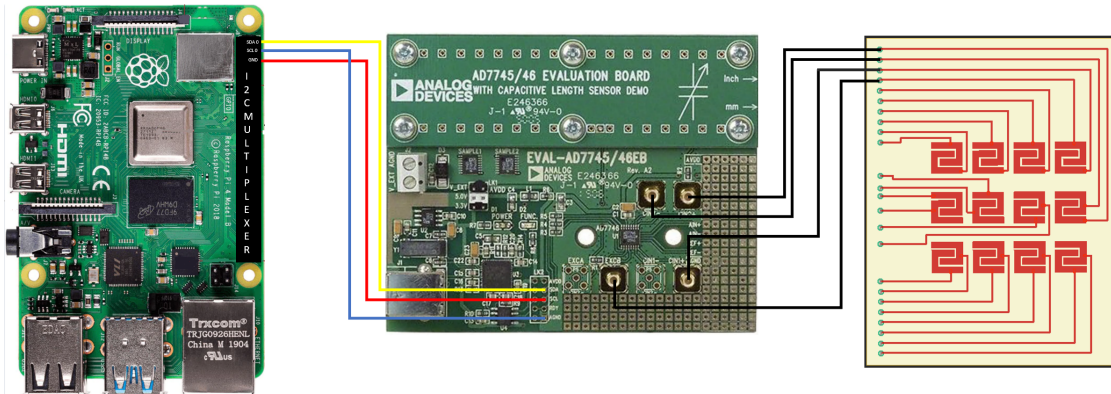


Figure 5.2: Scheme that presents how components must be connected.

### 5.2.1   Raspberry Pi 4

This device selects the chosen capacitor to collect data and it is responsible to store them in the correct table of the database. It will also be responsible for a TCP-IP connection to the webserver in order to provide data that allows the analysis of the acquired data. Figure 5.3 illustrates how the systems are connected.



Figure 5.3: Scheme with all components that allow the data acquisition and monitoring.

### 5.2.2   EVAL-AD7746

In the proposed architecture, twelve capacitors must be used. Each EVAL-AD7746 board (Figure 5.4) allows the acquisition of capacitance values from two capacitors, so six EVAL-AD7746 boards are required. The AD7746 architecture features an inherent

high resolution (24-bit no missing codes, up to 21-bit effective resolution), high linearity ($\pm0.01\%$) and high accuracy ($\pm4$ fF factory calibrated) [73].

The AD7746 provides a second capacitive channel, the CIN2. On the AD7746 evaluation board, the second capacitive channel is used with the on-board capacitive length sensor demo. To disable the capacitive length sensor demo, the two 0 $\Omega$ SMD resistors, R1 and R2, will be disconnected. Any capacitive sensor can then be directly interfaced to CIN2 of the AD7746 by connecting one end of the capacitive input to either the SMB connectors, labeled CIN2+ or CIN2−, and the other end to one of the SMB connectors, labeled EXCA or EXCB [73]. After concluding this alteration, it will be possible to connect two capacitors to the EVAL board.

Considering only one EVAL-AD7746, each planar electrode of the first capacitor must be connected using the channels CIN1+ (positive polarization) and EXCB (negative polarization), while the second must use the channels CIN2+ (positive polarization) and EXCA (negative polarization). The connection between the PCB and the EVAL-AD7746 board must be carried out by using the RG174 coaxial cable after a welding process.



Figure 5.4: EVAL-AD7746. [73]

Whenever it is necessary to collect a capacitance value, a write operation must be sent using I$^2$C protocol. This operation has the sequential values that must be written in each register, beginning in the address pointer 0x07. After sending the write message, it is necessary to send a read message. The latter indicates the registers that want to be read in order to obtain a capacitance value. This board requires the reading of three sequential values beginning in the address 0x01.

EVAL-AD7746 has a 5V power supply, so it can be connected directly to the USB port of a computer. However, the use of a USB multiplexer is required once six boards are used and the computer usually comprises fewer USB ports.

### 5.2.3 I$^2$C multiplexer

All the EVAL-AD7746 boards have the same slave address so it is impossible to connect all the I$^2$C communication cables directly to the Raspberry Pi since it would be impractical to select which one receives/sends a message. The use of an I$^2$C multiplexer can overcome this issue, once this device allows the connection of multiple I$^2$C devices with the same address to a single I$^2$C bus. The I$^2$C Multiplexer pHAT for Raspberry Pi (Figure 5.5)

not only allows the connection of eight devices with the same slave address, but also it enables the direct connection to a Raspberry Pi 4.



Figure 5.5: I$^2$C Multiplexer pHAT for Raspberry Pi (from *https://thepihut.com*).

## 5.3   Support platform

A support was designed according to the Figure 5.6. The description of each component is presented in the following topics and the technical drawings are in Appendix A.

1. Main support to stabilize all the components;

2. Polycarbonate sheet to prohibit bone-electrode contacts and ensure very high electrical resistivity. This electrically isolated sheet must be positioned above the sensors and below the bone samples;

3. Structure that must be clamped to the testing machine. The length of this structure was defined to minimize the influence of dielectrics on the metal grabs;

4. Bone fixation structure (that is attached with the element 3) to establish different distances between the bone samples and the interfacial sheet, where each bone sample was attached using nylon screws;

5. M5 screws to fix the polycarbonate plate;

6. Removable component, where the PCB will be incorporated;

7. Aluminium plate to ensure fixation to the compression machine, using M10 screws.
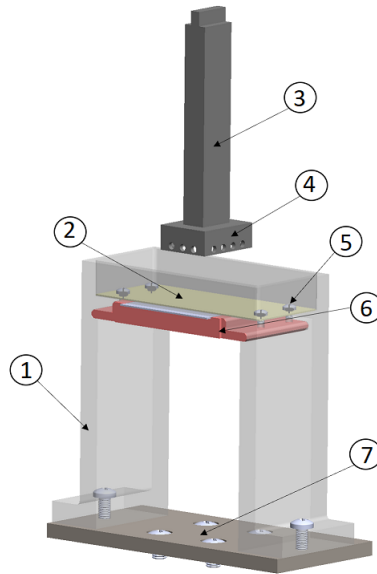
Figure 5.6: Support platform. The explanation of each component is in the previous page.

## 5.4   Bone samples

The experimental tests must be carried out with biological specimens, preferably porcine femur due to its similar characteristics to humans. After acquiring the samples, it is necessary to remove the cortical bone, the bone marrow and the remaining soft parts. Only the trabecular bone must be used in a total of six specimens with 20×10×8 mm.

## 5.5   Test machine

In order to carry out the experiment, it is necessary to move the bone samples downwards. The machine AGS−X 10 kN (Shimadzu) with a precision of 0.01 $\mu$m, must be used, being controlled with the software Trapezium X (Shimadzu).

## 5.6   Experimental procedure

The first step must be to configure the EVAL AD7746 to: (i) allow the data acquisition from two capacitors; (ii) define the monitoring sampling rate of 50 Hz; (iii) define the single-ended mode. These configurations must be carry out by sending the write operation trough the I$^2$C connection. The position $z=0$ must be the position where occurs the minimum bone-sheet bonding (when non-zero loads are detected).

After the initial settings, compression and decompression tests must be conducted. First, the bone must be displaced towards the capacitor without contact and the reverse path should also be performed. At each stop point (Figure 5.7) three hundred capacitance values must be acquired for each of the twelve capacitors.
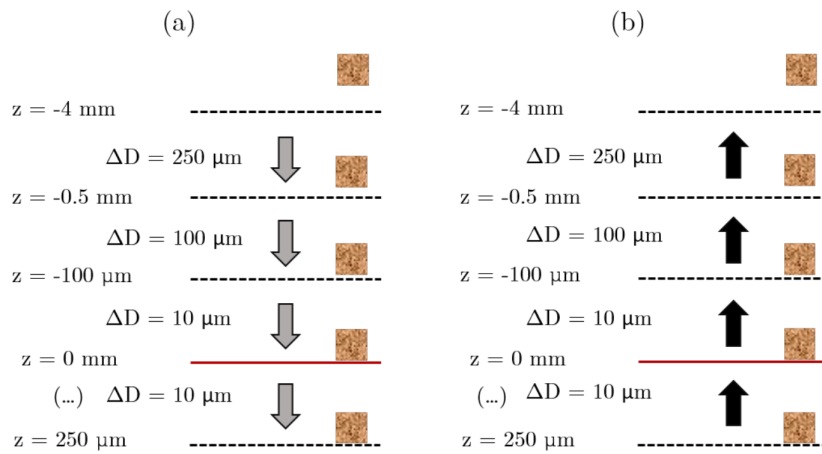
Figure 5.7: Scheme illustrating the compression and decompression test: a) compression b) decompression [67].

# Chapter 6

# Discussion

Aseptic loss represent the main reason for implant failure and this condition can lead to revision surgeries. The increasing number of patients that undergo this surgery emphasizes the need to significantly improve the sensing methods for efficient monitoring of the bone-implant fixation. The number of revision procedures may be minimized if the performance of sensing technologies is improved or innovative technologies emerge. Alternative methods of monitoring cementless implants were studied in the literature review. This study focused more on this type of implants due to the fact that the proposed architecture is designed for implants with this type of fixation.

A monitoring system will be effective if it fulfills the following criteria:

1. Operate non-invasively regarding peri-implants tissues;

2. Allow the integration inside implants;

3. Allow stretchable and flexible integration inside implants;

4. Allow their design with different topological structures and for different geometries of the bone-implant interface;

5. Enable controllable and personalized monitoring of target regions on the tissues;

6. Allow to follow-up the bone-implant interface state throughout the daily life of patients.

Considering the technologies studied in the literature review and the criteria presented above, the following table 6.1, adapted from Cachão *et al.* [38], identifies the ability of each technology to provide an effective monitoring of the bone-implant fixation.

Table 6.1: Criteria used to define the potential of monitoring methods. Adapted from Cachão *et al.* [38]

| Methodologies | Methods | Requirements | | | | | |
|---|---|---|---|---|---|---|---|
| | | 1 | 2 | 3 | 4 | 5 | 6 |
| Vibrometric | Ext. mechanical excitation / Ext. mechanical signal | ✓ | × | × | ✓ | × | ✓ |
| | Ext. magnetic induction / Ext. mechanical signal | ✓ | ✓ | × | ✓ | × | ✓ |
| | Int. mechanical excitation / Ext. mechanical signal | ✓ | × | × | ✓ | × | ✓ |
| Acoustic | Ext. mechanical excitation / Ext. acoustic signal | ✓ | × | × | ✓ | × | ✓ |
| | Int. mechanical excitation / Ext. acoustic signal | ✓ | × | × | ✓ | × | ✓ |
| | Ext. magnetic induction / Ext. acoustic signal | ✓ | ✓ | × | ✓ | × | ✓ |
| Bioeletrical impedance | Ext. electrical current / Ext. electric potential difference | ✓ | × | × | ✓ | × | ✓ |
| Magnetic induction | Ext. magnetic induction / Ext. magnetic induction | ✓ | ✓ | × | ✓ | × | ✓ |
| Strain | Int. mechanical loads / Int. bone deformation | × | ✓ | ✓ | ✓ | × | ✓ |
| | Int. mechanical loads / Int. fixation plate deformation | ✓ | ✓ | ✓ | ✓ | × | ✓ |
| Capacitance | Intracorporeal dielectric alteration / Intracorporeal capacitance change | ✓ | ✓ | ✓ | ✓ | ✓ | ✓ |

Terminology: Int.- Intracorporeal; Ext. - Extracorporeal

Vibrometric and acoustic methods are the most studied methodologies up to date. The most relevant limitations of these studies is not only the impossibility of allowing stretchable and flexible integration, but also the unfeasibility of monitoring target regions. Another point to note is that although they enable continuous patient monitoring, it can be uncomfortable due to the use of extracorporeal systems.

The methodology based on bioeletrical impedance operates non-invasively regarding peri-implants tissues and can be used in different geometries of the bone-implant interface. However, the integration inside the implant and the monitoring of target regions are hard to achieve.

In the methodology based on magnetic induction, the limitations are related to being hard to implement stretchable and flexible sensors integration inside implants and the difficulty of monitoring target regions. It should be noted that only one method was proposed for this methodology and that four of the six requirements necessary to be considered an ideal implant are fulfilled.

In the strain approach, two methodologies were proposed and the common limitation is their current inability to monitor target peri-implant regions.

Capacitive methodologies, which is within the scope of the technology here proposed, fulfill all the requirements for an effective monitoring.

Briefly, as shown in Table 7.1, the main limitations of the studied methods remain the difficult incorporation of the systems inside the implant and the inability to evaluate specific areas of the bone-implant interface. Another essential point to highlight is that although all of the methods can monitor the bone-implant interface states during the patient's daily life, the proposed systems can be uncomfortable to use and reduce the quality of life of the patients.

The main characteristics that distinguish this prototype from the others already studied as a capacitive approach are: (i) three capacitive architecture were include and their dimensions can be easily altered if necessary; (ii) the number of capacitors can be adjusted, in multiples of three and the website will work in the same manner; (iii) allows the monitoring of different target regions; (iv) bone-sensor distances may be acquired during the daily life of the patient.

It should be noted that the possibility of continuously monitoring the bone-implant interface will not be inconvenient for the patient since the system is incorporated within the implant. The website allows a proximity between the clinician and the patient, which is very important for an effective monitoring and ensuring the reduced number of medical appointments.

The analysis by region proved to be advantageous so that, in the future, bone growth stimulation could be performed only in regions were bone loss was detected.

With the simulation of the approximation test, it is possible to verify that small changes in distance are also visible in both graphs, which demonstrates the potential of the proposed system in experimental tests.

The possibility of downloading the file that comprises all the acquired data is quite useful to effectively track the bone-implant fixation, allows a more accurate analysis of small variations of displacement and allows the elaboration of other type of studies.

Even if this system provides several advances in the proposed monitoring systems, it also has some limitations such as the memory needed to save data, in particular if the primary surgery is made in young people. This problematic can be solved if the tables in the database host in the Raspberry Pi are truncate after downloading the Excel file. In order to be fully functional and to be able to establish a TCP/IP communication, this system requires electric energy which can only be obtained using effective energy harvesting systems incorporated within the bioelectronic implants.

# Chapter 7

# Conclusion and Future Works

There are currently several studies that have identified several methods for monitoring the bone-implantinterface: vibrometric, acoustic, bioelectric impedance, magnetic induction, strain and capacitance. Although more than twenty four technologies were already proposed, none is able to provide an effective monitoring. This work aims to contribute to this development, designing an advanced technology that provides the following breakthroughs: (i) network of cosurface capacitors to acquire data from chosen regions, in order to reconstruct the bone-implant fixation state in a three dimensional plot; (ii) data can be acquired from target regions in order to proceed to a separate analysis; (iii) data can be acquired continuously during a period of time or can be acquired at a specific moment.

It was not possible to carry out experimental tests, so simulation tests were performed using capacitance values generated from data acquired during previous experimental tests *in vitro*. The prototype for the experimental tests was designed and instructions were given on how the different components must be electrically interconnected.

The results obtained in the two performed simulation tests demonstrate the potential of the website to operate together with a network-based corsurface capacitive sensing prototype, which must be manufactured in future works, as well as to validate the concept of bioelectronic implant extracorporeally controlled by clinicians.

As revision surgeries must be minimized to improve the quality of life of patients, research efforts must be conducted to design an effective instrumented implant. In this sense, the following future works are proposed:

- To conduct experimental tests *in vitro* and *in vivo* to validate the network-based sensing system here proposed;

- To miniaturize the overall data acquisition system;

- Development of a Master-Slave system (hardware and software) with ability to wirelessly: (i) switch between stimulation and sensing operations; (ii) configure and operate both the delivery of electric stimuli and the monitoring of bone-implant fixation state;

- Conducting experimental tests *in vitro* and *in vivo* using other biophysical sensors;

- Publish of a scientific paper with the obtained results.

# Bibliography

[1] Robert Pivec, Aaron J. Johnson, Simon C. Mears, and Michael A. Mont. Hip arthroplasty. *The Lancet*, 380(9855):1768–1777, 2012.

[2] G Labek, M Thaler, W Janda, M Agreiter, B Stöckl, and Orthopaedic Surgeon. Revision rates after total joint replacement cumulative results from worldwide joint register datasets. *J Bone Joint Surg [Br]*, pages 93–293, 2011.

[3] Marco P.Soares Dos Santos, Ana Marote, T. Santos, João Torrão, A. Ramos, José A.O. Simões, Odete A.B. Da Cruz E Silva, Edward P. Furlani, Sandra I. Vieira, and Jorge A.F. Ferreira. New cosurface capacitive stimulators for the development of active osseointegrative implantable devices. *Scientific Reports*, 6, jul 2016.

[4] Yousef Abu-Amer, Isra Darwech, and John C. Clohisy. Aseptic loosening of total joint replacements: Mechanisms underlying osteolysis and potential therapies, jun 2007.

[5] Steven Kurtz, Kevin Ong, Edmund Lau, Fionna Mowat, and Michael Halpern. Projections of primary and revision hip and knee arthroplasty in the United States from 2005 to 2030. *Journal of Bone and Joint Surgery - Series A*, 89(4):780–785, 2007.

[6] Andrew J. Carr, Otto Robertsson, Stephen Graves, Andrew J. Price, Nigel K. Arden, Andrew Judge, and David J. Beard. Knee replacement. *The Lancet*, 379(9823):1331–1340, 2012.

[7] Steven M. Kurtz, Edmund Lau, Kevin Ong, Ke Zhao, Michael Kelly, and Kevin J. Bozic. Future young patient demand for primary and revision joint replacement: National projections from 2010 to 2030. In *Clinical Orthopaedics and Related Research*, volume 467, pages 2606–2612. Springer New York, 2009.

[8] Peter M. Brooks. Impact of osteoarthritis on individuals and society: How much disability? Social consequences and health economic implications. *Current Opinion in Rheumatology*, 14(5):573–577, 2002.

[9] Ali Guermazi, Jingbo Niu, Daichi Hayashi, Frank W. Roemer, Martin Englund, Tuhina Neogi, Piran Aliabadi, Christine E. McLennan, and David T. Felson. Prevalence of abnormalities in knees detected by MRI in adults without knee osteoarthritis: Population based observational study (Framingham Osteoarthritis Study). *BMJ (Online)*, 345(7874), sep 2012.

[10] S. Oussedik and F. Haddad. Further doubts over the performance of treatment centres in providing elective orthopaedic surgery. *Journal of Bone and Joint Surgery - Series B*, 91(9):1125–1126, 2009.

[11] Marco P. Soares dos Santos, Jorge A.F. Ferreira, A. Ramos, José A.O. Simões, Raul Morais, Nuno M. Silva, Paulo M. Santos, M. J.C.S. Reis, and T. Oliveira. Instrumented hip implants: Electric supply systems. *Journal of Biomechanics*, 46(15):2561–2571, 2013.

[12] Rory J. Ferguson, Antony JR Palmer, Adrian Taylor, Martyn L. Porter, Henrik Malchau, and Sion Glyn-Jones. Hip replacement. *The Lancet*, 392(10158):1662–1671, 2018.

[13] Robert Pivec, Aaron J. Johnson, Simon C. Mears, and Michael A. Mont. Hip arthroplasty. *The Lancet*, 380(9855):1768–1777, 2012.

[14] Andrew J. Carr, Otto Robertsson, Stephen Graves, Andrew J. Price, Nigel K. Arden, Andrew Judge, and David J. Beard. Knee replacement. *The Lancet*, 379(9823):1331–1340, 2012.

[15] Robin Brittain, Elaine Young, Victoria Mccormack, and Mike Swanson. 16th Annual Report 2019:National Joint Registry for England, Wales, Northern Ireland and the Isle of Man. (December 2018), 2019.

[16] Go Yamako, Etsuo Chosa, Koji Totoribe, Shinji Watanabe, and Takero Sakamoto. Trade-off between stress shielding and initial stability on an anatomical cementless stem shortening: In-vitro biomechanical study. *Medical Engineering and Physics*, 37(8):820–825, aug 2015.

[17] J Davis. Overview of Biomaterials and Their Use in Medical Devices. Technical report, 2003.

[18] C. Pabinger and A. Geissler. Utilization rates of hip arthroplasty in OECD countries. *Osteoarthritis and Cartilage*, 22(6):734–741, 2014.

[19] Richard A. Brand, Michael A. Mont, and M. M. Manring. Biographical sketch: Themistocles Gluck (1853-1942). *Clinical Orthopaedics and Related Research*, 469(6):1525–1527, 2011.

[20] M. Navarro, A. Michiardi, O. Castaño, and J. A. Planell. Biomaterials in orthopaedics. *Journal of the Royal Society Interface*, 5(27):1137–1158, 2008.

[21] Qizhi Chen and George A. Thouas. Metallic implant biomaterials. *Materials Science and Engineering R: Reports*, 87:1–57, 2015.

[22] Saverio Affatato, Alessandro Ruggiero, and Massimiliano Merola. Advanced biomaterials in hip joint arthroplasty. A review on polymer and ceramics composites as alternative bearings. *Composites Part B: Engineering*, 83:276–283, 2015.

[23] Stephen Richard Knight, Randeep Aujla, and Satya Prasad Biswas. 100 Years of Operative History Er Ci Us E on Er Al. *Orthopaedic Reviews*, 3:2–4, 2011.

[24] Reijo Lappalainen and Seppo S. Santavirta. Potential of coatings in total hip replacement. *Clinical Orthopaedics and Related Research*, (430):72–79, 2005.

[25] N. W. Rydell. Forces acting on the femoral head-prosthesis. A study on strain gauge supplied prostheses in living persons. *Acta Orthopaedica Scandinavica*, 37, 1966.

[26] Georg Bergmann, Friedmar Graichen, Jörn Dymke, Antonius Rohlmann, Georg N. Duda, and Philipp Damm. High-tech hip implant for wireless temperature measurements in vivo. *PLoS ONE*, 7(8), aug 2012.

[27] G. Bergmann, F. Graichen, and A. Rohlmann. Hip joint forces in sheep. *Journal of Biomechanics*, 1999.

[28] Friedmar Graichen, Georg Bergmann, and Antonius Rohlmann. Hip endoprosthesis for in vivo measurement of joint force and temperature. *Journal of Biomechanics*, 32(10):1113–1117, 1999.

[29] Philipp Damm, Friedmar Graichen, Antonius Rohlmann, Alwina Bender, and Georg Bergmann. Total hip joint prosthesis for in vivo measurement of forces and moments. *Medical Engineering and Physics*, 32(1):95–100, 2010.

[30] Marco P. Soares Dos Santos, Jorge A.F. Ferreira, A. Ramos, and José A.O. Simões. Active orthopaedic implants: Towards optimality. *Journal of the Franklin Institute*, 352(3):813–834, 2015.

[31] Susan. Standring, Neil R. Borley, and Henry Gray. *Gray's anatomy: the anatomical basis of clinical practice*. Churchill Livingstone/Elsevier, 2008.

[32] António Completo and Fonseca Fernando. *Fundamentos de Biomecânica-Musculo Esqueletica e Ortopedica*. PubIndustria, 2011.

[33] Ulf H. Lerner. Osteoblasts, Osteoclasts, and Osteocytes: Unveiling Their Intimate-Associated Responses to Applied Orthodontic Forces. *Seminars in Orthodontics*, 18(4):237–248, 2012.

[34] Hussein AI Morgan EF, Unnikrisnan GU. Bone Mechanical Properties in Healthy and Diseased States. *Annu Rev Biomed Eng.*, 20:119–143, 2018.

[35] C. Gabriel, S. Gabriel, and E. Corthout. The dielectric properties of biological tissues: I. Literature survey. *Physics in Medicine and Biology*, 41(11):2231–2249, 1996.

[36] Cathérine Ruther, Christian Schulze, Andrea Boehme, Hannes Nierath, Hartmut Ewald, Wolfram Mittelmeier, Rainer Bader, and Daniel Kluess. Investigation of a passive sensor array for diagnosis of loosening of endoprosthetic implants. *Sensors (Switzerland)*, 13(1):1–20, 2013.

[37] Shiying Hao, John T. Taylor, Chris R. Bowen, Sabina Gheduzzi, and Anthony W. Miles. Sensing methodology for in vivo stability evaluation of total hip and knee arthroplasty. *Sensors and Actuators, A: Physical*, 2010.

[38] João Henrique Cachão, Marco P.Soares Dos Santos, Rodrigo Bernardo, António Ramos, Rainer Bader, Jorge A.F. Ferreira, António Torres Marques, and José A.O. Simões. Altering the course of technologies to monitor loosening states of endoprosthetic implants. *Sensors (Switzerland)*, 20(1):7–10, 2020.

[39] Yongde Zhang, Aaron W. Putnam, Anneliese D. Heiner, John J. Callaghan, and Thomas D. Brown. Reliability of detecting prosthesis/cement interface radiolucencies in total hip arthroplasty. *Journal of Orthopaedic Research*, 20(4):683–687, 2002.

[40] D.M. Mulcahy, G.C.C. Fenelon, and D.P. McInerney. Aspiration arthrography of the hip joint. *The Journal of Arthroplasty*, 11(1):64–68, 1996.

[41] A. Blum, J. B. Meyer, A. Raymond, M. Louis, O. Bakour, R. Kechidi, A. Chanson, and P. Gondim-Teixeira. CT of hip prosthesis: New techniques and new paradigms. *Diagnostic and Interventional Imaging*, 97(7-8):725–733, 2016.

[42] H. John Cooper, Amar S. Ranawat, Hollis G. Potter, Li Foong Foo, Shari T. Jawetz, and Chitranjan S. Ranawat. Magnetic Resonance Imaging in the Diagnosis and Management of Hip Pain After Total Hip Arthroplasty. *Journal of Arthroplasty*, 24(5):661–667, 2009.

[43] Leif Claassen, Max Ettinger, Christian Plaass, Kiriakos Daniilidis, Tilman Calliess, and Marco Ezechieli. Diagnostic value of bone scintigraphy for aseptic loosening after total knee arthroplasty. *Technology and Health Care*, 22(5):767–773, 2014.

[44] A. P. Georgiou and J. L. Cunningham. Accurate diagnosis of hip prosthesis loosening using a vibrational technique. *Clinical Biomechanics*, 16(4):315–323, 2001.

[45] Abdullah A. Alshuhri, Timothy P. Holsgrove, Anthony W. Miles, and James L. Cunningham. Development of a non-invasive diagnostic technique for acetabular component loosening in total hip replacements. *Medical Engineering and Physics*, 37(8):739–745, 2015.

[46] Abdullah A. Alshuhri, Timothy P. Holsgrove, Anthony W. Miles, and James L. Cunningham. Non-invasive vibrometry-based diagnostic detection of acetabular cup loosening in total hip replacement (THR). *Medical Engineering and Physics*, 48:188–195, 2017.

[47] Johannes Sebastian Rieger, Sebastian Jaeger, Christian Schuld, Jan Philippe Kretzer, and Rudi Georg Bitsch. A vibrational technique for diagnosing loosened total hip endoprostheses: An experimental sawbone study. *Medical Engineering and Physics*, 35(3):329–337, 2013.

[48] Johannes S. Rieger, Sebastian Jaeger, Jan Philippe Kretzer, Rüdiger Rupp, and Rudi G. Bitsch. Loosening detection of the femoral component of hip prostheses with extracorporeal shockwaves: A pilot study. *Medical Engineering and Physics*, 37(2):157–164, 2015.

[49] Maurizio Lannocca, Elena Varini, Angelo Cappello, Luca Cristofolini, and Ewa Bialoblocka. Intra-operative evaluation of cementless hip implant stability: A

prototype device based on vibration analysis. *Medical Engineering and Physics*, 29(8):886–894, 2007.

[50] Elena Varini, Ewa Bialoblocka-Juszczyk, Maurizio Lannocca, Angelo Cappello, and Luca Cristofolini. Assessment of implant stability of cementless hip prostheses through the frequency response function of the stem-bone system. *Sensors and Actuators, A: Physical*, 163(2):526–532, 2010.

[51] Leonard C. Pastrav, Siegfried Vn Jaecques, Ilse Jonkers, Georges Van Der Perre, and Michiel Mulier. In vivo evaluation of a vibration analysis technique for the per-operative monitoring of the fixation of hip prostheses. *Journal of Orthopaedic Surgery and Research*, 4(1):1–10, 2009.

[52] Ching Chuan Jiang, Ju Hong Lee, and Tung Tai Yuan. Vibration arthrometry in thé patients with failed total knee replacement. *IEEE Transactions on Biomedical Engineering*, 47(2):219227, 2000.

[53] Cathérine Ruther, Hannes Nierath, Hartmut Ewald, James L. Cunningham, Wolfram Mittelmeier, Rainer Bader, and Daniel Kluess. Investigation of an acoustic-mechanical method to detect implant loosening. *Medical Engineering and Physics*, 35(11):1669–1675, 2013.

[54] Catherine Ruther, Ulrich Timm, Andreas Fritsche, Hartmut Ewald, Wolfram Mittelmeier, Rainer Bader, and Daniel Kluess. A New Approach for Diagnostic Investigation of Total Hip Replacement Loosening. *Communications in Computer and Information Science*, 273:74–79, 2011.

[55] Diana Glaser, Richard D. Komistek, Harold E. Cates, and Mohamed R. Mahfouz. A non-invasive acoustic and vibration analysis technique for evaluation of hip joint conditions. *Journal of Biomechanics*, 43(3):426–432, 2010.

[56] Richard A. Kapur. Acoustic emission in orthopaedics: A state of the art review. *Journal of Biomechanics*, 49(16):4065–4072, 2016.

[57] A. C. Unger, H. Cabrera-Palacios, A. P. Schulz, Ch Jürgens, and Andreas Paech. Acoustic monitoring (RFM) of total hip arthroplasty results of a cadaver study. *European Journal of Medical Research*, 14(6):264–271, 2009.

[58] Quentin Goossens, Steven Leuridan, Petr Henyš, Jorg Roosen, Leonard Pastrav, Michiel Mulier, Wim Desmet, Kathleen Denis, and Jos Vander Sloten. Development of an acoustic measurement protocol to monitor acetabular implant fixation in cementless total hip Arthroplasty: A preliminary study. *Medical Engineering and Physics*, 49:28–38, 2017.

[59] Diana Glaser, Richard D. Komistek, Harold E. Cates, and Mohamed R. Mahfouz. Clicking and squeaking: In vivo correlation of sound and separation for different bearing surfaces. *Journal of Bone and Joint Surgery - Series A*, 90(SUPPL. 4):112–120, 2008.

[60] Hartmut Ewald, Ulrich Timm, Rainer Bader, and Daniel Kluess. Acoustic sensor system for loosening detection of hip implants. pages 494–497, 2011.

[61] Hartmut Ewald, Cathérine Ruther, Wolfram Mittelmeier, and Rainer Bader. A novel in vivo Sensor for Loosening Diagnostics in Total Hip Replacement. 2011.

[62] Pasquale Arpaia, Fabrizio Clemente, and Antonio Zanesco. Low-invasive diagnosis of metallic prosthesis osseointegration by electrical impedance spectroscopy. *IEEE Transactions on Instrumentation and Measurement*, 56(3):784–789, 2007.

[63] Pasquale Arpaia, Fabrizio Clemente, and Carmine Romanucci. In-vivo test procedure and instrument characterization for EIS-based diagnosis of prosthesis osseointegration. *Conference Record - IEEE Instrumentation and Measurement Technology Conference*, pages 1–6, 2007.

[64] Hartmut Ewald, Cathérine Ruther, Wolfram Mittelmeier, Rainer Bader, and Daniel Kluess. A novel in vivo sensor for loosening diagnostics in total hip replacement. *Proceedings of IEEE Sensors*, 133(1):89–92, 2011.

[65] Andrew R. Burton, Peng Sun, and Jerome P. Lynch. Bio-compatible wireless inductive thin-film strain sensor for monitoring the growth and strain response of bone in osseointegrated prostheses. *Structural Health Monitoring*, 2019.

[66] Kirk C. McGilvray, Emre Unal, Kevin L. Troyer, Brandon G. Santoni, Ross H. Palmer, Jeremiah T. Easley, Hilmi Volkan Demir, and Christian M. Puttlitz. Implantable microelectromechanical sensors for diagnostic monitoring and post-surgical prediction of bone fracture healing. *Journal of Orthopaedic Research*, 33(10):1439–1446, 2015.

[67] Luís Miguel Amaral Henriques. *Sistema de monitorização capacitivo para implantes ósseos instrumentados*. Master thesis, Universidade de Aveiro, 2018.

[68] R. Puers, M. Catrysse, G. Vandevoorde, R. J. Collier, E. Louridas, F. Burny, M. Donkerwolcke, and F. Moulart. Telemetry system for the detection of hip prosthesis loosening by vibration analysis. *Sensors and Actuators, A: Physical*, 85(1):42–47, 2000.

[69] U. Marschner, H. Grätz, B. Jettkant, D. Ruwisch, G. Woldt, W. J. Fischer, and B. Clasbrummel. Integration of a wireless lock-in measurement of hip prosthesis vibrations for loosening detection. *Sensors and Actuators, A: Physical*, 156(1):145–154, 2009.

[70] Sebastian Sauer and Uwe Marschner. Medical wireless vibration measurement system for hip prosthesis loosening detection. *SENSORDEVICES, The Third International Conference on Sensor Device Technologies and Applications Applications (2012)*, (c):9–13, 2012.

[71] Django Documentation. https://docs.djangoproject.com.

[72] Rodrigo Bernardo. *Sistema híbrido indutivo-capacitivo para operações de estimulação e monitorização em implantes ósseos instrumentados*. Master thesis, Universidade de Aveiro, 2019.

[73] Analog Devices. AD7746 Evaluation Board. 2005.

# Appendices
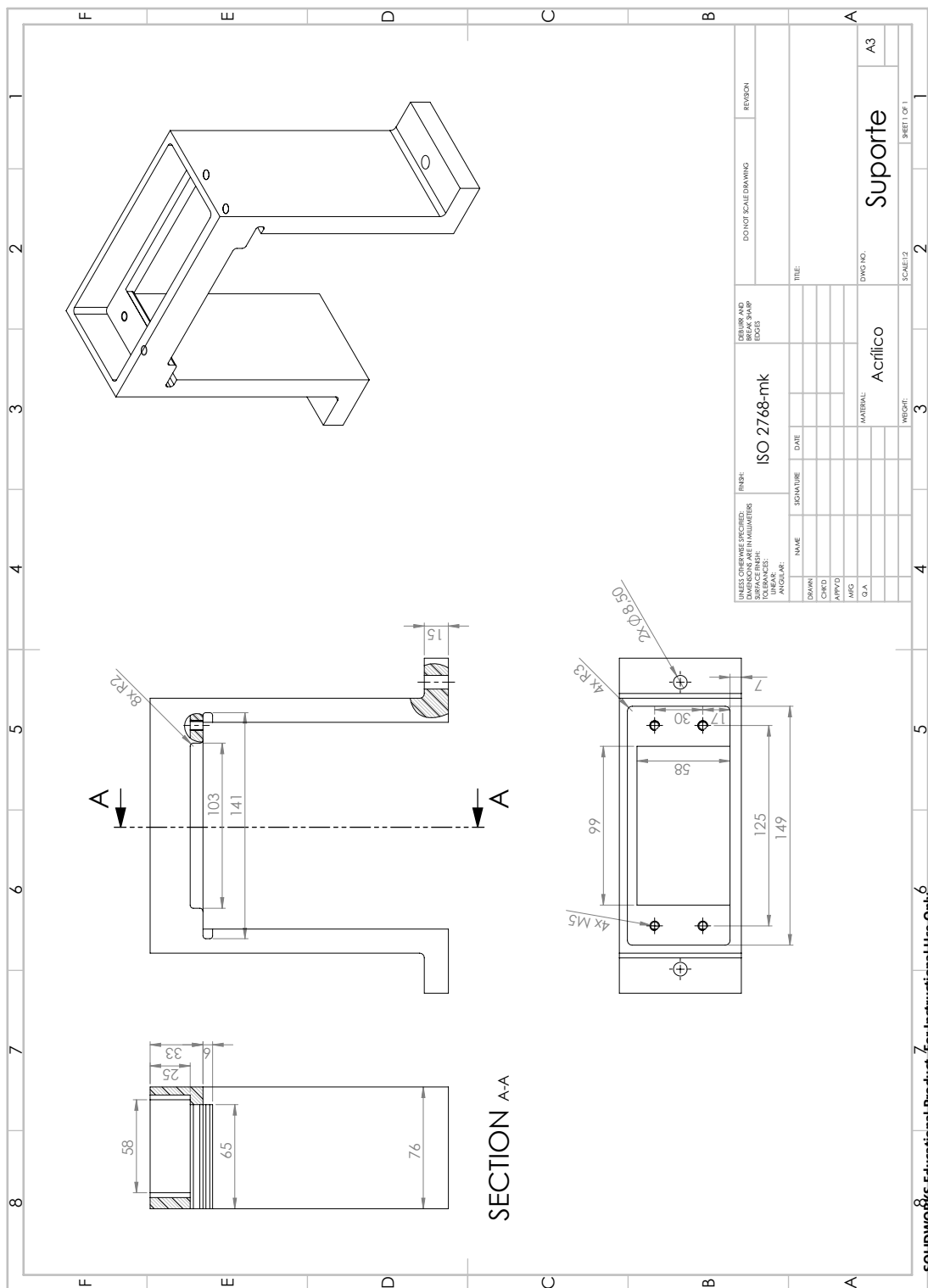
# Appendix A

# Technical drawings

Figure A.1: Technical drawing of the principal support for the experimental setup.

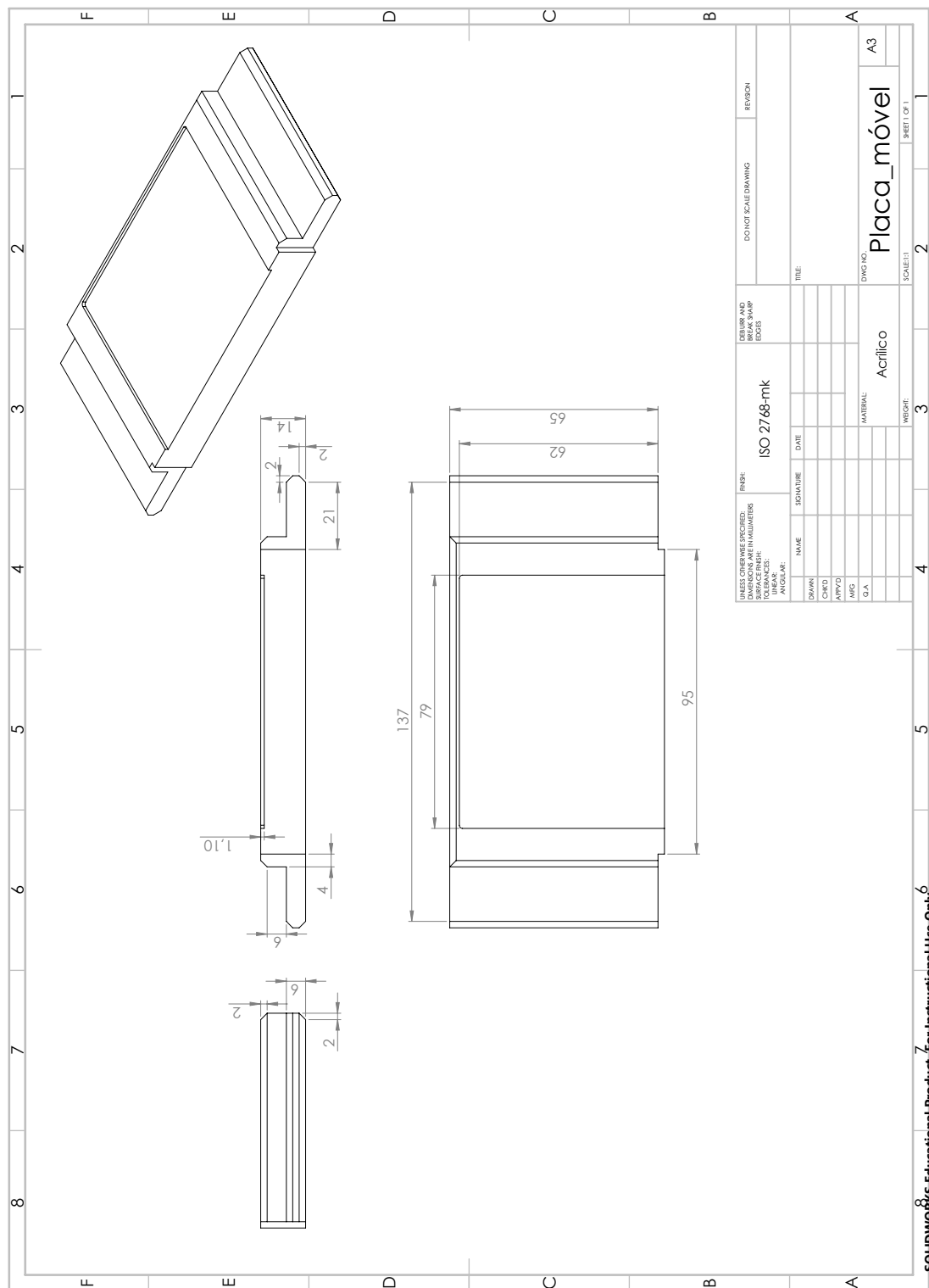Figure A.2: Technical drawing of the bone support for the experimental setup.

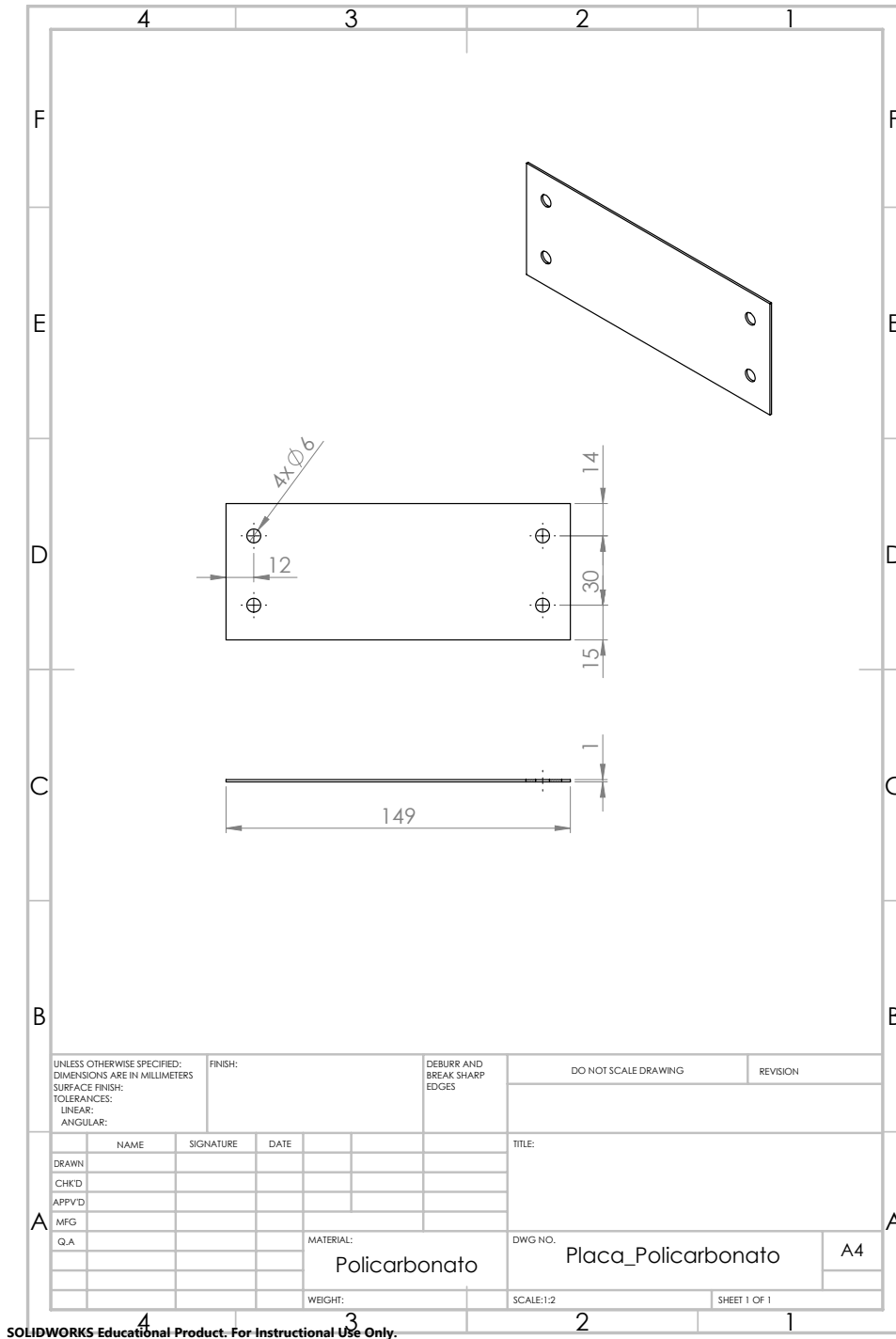Figure A.3: Technical drawing of the capacitor support for the experimental setup.

Figure A.4: Technical drawing of the contact plate between the bone and the capacitor for the experimental setup.
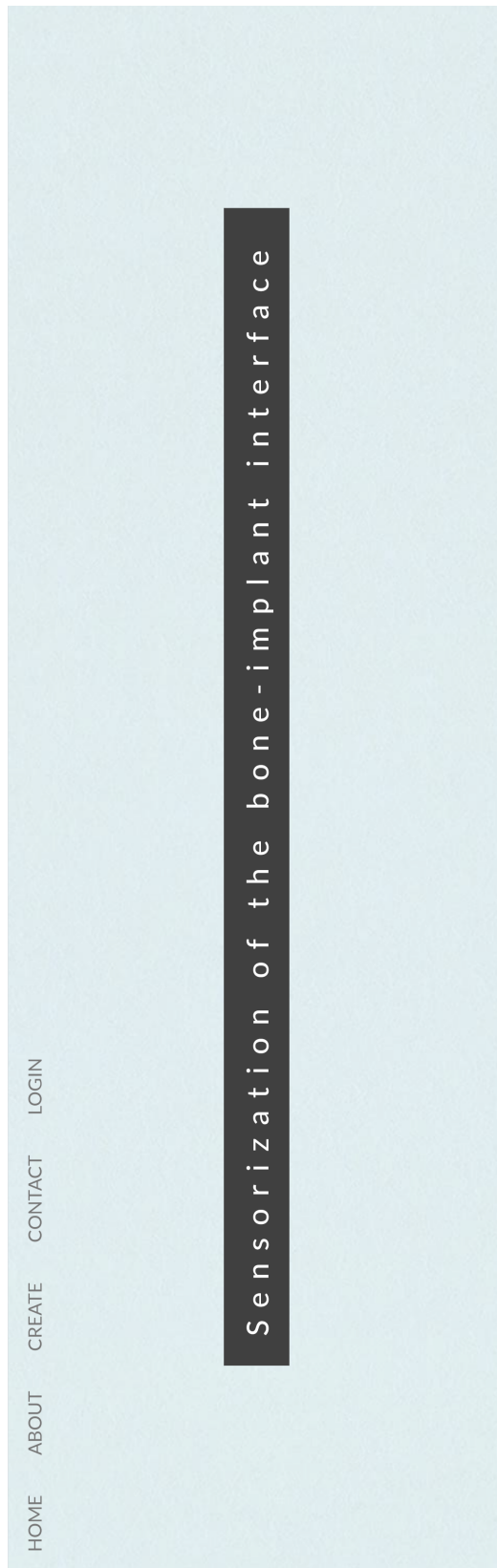
# Appendix B

# Website

HOME ABOUT CREATE CONTACT LOGIN

**Sensorization of the bone-implant interface**

ABOUT

Arthroplasties, which consist in a reconstructive procedure that alters the structure of a joint, are one of the most common surgical procedures performed worldwide, accounted for more than a million replacement surgeries every year. This number is expected to double in the next two decades, due to the ageing population and obesity. Although this surgery has excellent outcomes, revision surgery is still necessary in 6.45% of the cases after five years and 12.9% after ten years. Surgical revision of joint replacement are more complex and invasive than the primary replacements. Bone loss is an anomaly that leads to unstable bone-implant fixations. Aseptic loss is the main reason for implant failure that occurs

Figure B.1: Home page.

HOME      ABOUT      CREATE      CONTACT      LOGIN

## ABOUT

Arthroplasties, which consist in a reconstructive procedure that alters the structure of a joint, are one of the most common surgical procedures performed worldwide, accounted for more than a million replacement surgeries every year. This number is expected to double in the next two decades, due to the ageing population and obesity. Although this surgery has excellent outcomes, revision surgery is still necessary in 6.45% of the cases after five years and 12.9% after ten years. Surgical revision of joint replacement are more complex and invasive than the primary replacements. Bone loss is an anomaly that leads to unstable bone-implant fixations. Aseptic loss is the main reason for implant failure that occurs when adverse bone remodelling due to stress-shielding. In cementless implants, aseptic loosening results of inadequate initial fixation or biologic loss of fixation caused by particle-induced osteolysis around the implant. Many efforts have been performed to study this issue and new implant technologies emerged in the scientific community.

In order to combat this problematic and reduce the number of revision surgeries, a recent concept of instrumented implant is proposed, which has a network of capacitors continuously acquiring data and releasing it to a database. Thus, it is possible to assess the fixation status before proceeding to a revision surgery. After primary surgery, the clinician must create an account on this website. In order to do that, the clinician has to define an username, a password and the patient's name and the surname, since the same username can be associated with multiple patients.

Figure B.2: About section.

# CREATE AN ACCOUNT

*For remote control*

The number and the type of capacitors used have to be specified. The type of capacitor is stated according to the nomenclature shown in the picture on the left. The Time Sampling accounts for the days between the intended acquisitions. The number of acquisitions intended corresponds to the total number of acquisitions that must be done before converting the mean value into a bone-imlpant distance.

HOME    ABOUT    CREATE    CONTACT    LOGIN

a       b       c

Username
Password
Patient
No Acquis.

Capacitor Type
No. Capacitors
Time Sampling
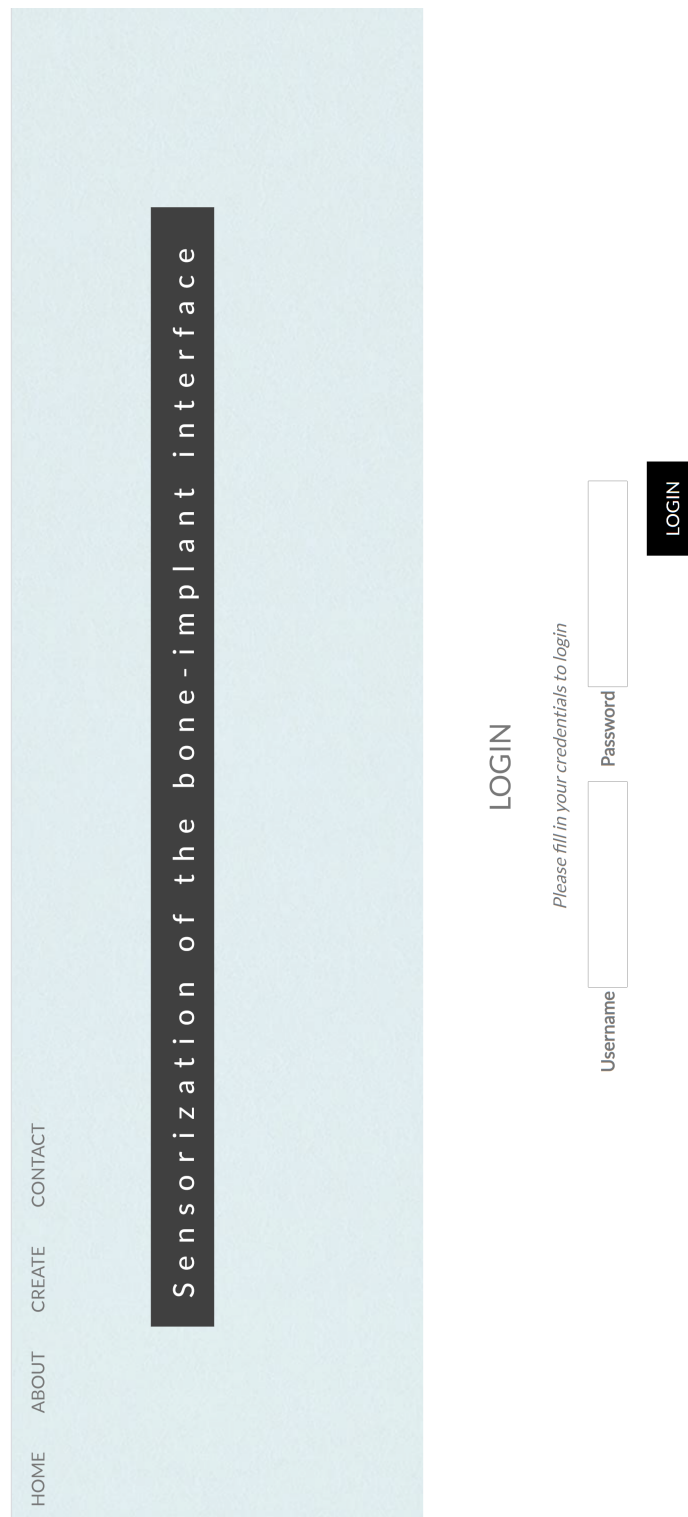IP Identifier

Create

Figure B.3: Create section.

Figure B.4: Contact section.

Figure B.5: Login page.

Figure B.6: Control page.